Experimental investigations of the preservation/degradation of microbial signatures in the presence of clay minerals under Martian subsurface conditions

Isis Criouet, Jean-Christophe Viennet, Etienne Balan, Fabien Baron, Arnaud Buch, Fériel Skouri-Panet, Maxime Guillaumet, Ludovic Delbes, Laurent Remusat, Sylvain Bernard

EXPERIMENTAL INVESTIGATIONS OF THE PRESERVATION/DEGRADATION OF MICROBIAL SIGNATURES IN THE PRESENCE OF CLAY MINERALS UNDER MARTIAN SUBSURFACE CONDITIONS

Isis Criouet [1], Jean-Christophe Viennet [1,2]., Etienne Balan [1], Fabien Baron [3], Arnaud Buch [4], Fériel Skouri-Panet [1], Maxime Guillaumet [1], Ludovic Delbes [1], Laurent Remusat [1], Sylvain Bernard [1]

[1] Muséum National d'Histoire Naturelle, Sorbonne Université, UMR CNRS 7590, Institut de minéralogie, de physique des matériaux et de cosmochimie, Paris, France
[2] Univ. Lille, CNRS, INRA, ENSCL, UMR 8207 - UMET - Unité Matériaux et Transformations, F-59000 Lille, France
[3] Institut de Chimie des Milieux et Matériaux de Poitiers (IC2MP), UMR 7285 CNRS, Université de Poitiers, F-86073 Poitiers Cedex 9, France
[4] Laboratoire Génie des Procédés et Matériaux, CentraleSupélec, Gif-sur-Yvette, France

ABSTRACT

The astrobiological exploration of Mars is ongoing. Ancient Martian terrains covered by clay minerals are seen as the most promising targets to search for biosignatures as clay minerals are believed to have a high potential for biopreservation. Here, we experimentally investigate the biopreservation potential of saponite, a Mg-rich smectite, relying on series of experiments conducted with mixtures of *E. coli* cells and saponite exposed to thermal conditions (up to 200°C) for different durations (up to 100 days) under a Martian atmosphere (CO_2) in the presence of water, thereby simulating episodes of fluid circulation typical of those periodically occurring on Mars. Residues were characterized using elemental analyses, mid-infrared (Mid-IR) spectroscopy and X-ray diffraction (XRD) to document the chemistry of the residual organic materials as well as the nature and crystallinity of the residual mineral materials. Results show that saponite may delay the chemical degradation of some organic materials by selectively trapping N-rich organic compounds within its interlayer space. However, such trapping of N-rich organic compounds does not completely protect them from degradation with increasing temperature and experimental duration, as shown by the N/C ratio, $\delta^{13}C$ values, Mid-IR spectra and XRD patterns of the residues of experiments conducted at 200°C or at 150°C for 100 days. This suggests that saponite is not that efficient in protecting biogenic organic compounds from thermal degradation over long periods of time. Altogether, the present study provides information on what can be found (and thus pinpointing what should be searched for) in the ancient Martian geological record.

KEYWORDS

Biosignatures, Mars, Clay minerals, Smectites, Laboratory experiments

1. INTRODUCTION

All cases made for Martian biosignatures have been challenged so far (Sinton, 1957, 1959; Levin and Straat, 1977; McKay et al., 1996; McSween, 2019), but the consensus is that Life may have existed on Mars. Today, the surface of Mars is globally not habitable: it is cold, dry, and continuously exposed to biologically harmful radiation. Any organic material existing at the very surface of Mars (*i.e.* the first mm) would rapidly be destroyed by intense non-ionizing and ionizing radiation (i.e. UVs, galactic cosmic rays, solar energetic particles - Hassler et al., 2014; Fornaro et al., 2018; Fox et al., 2019; Megevand et al., 2021). But things were different during the Noachian (4.1 to 3.7 Ga): environments likely existed with liquid water and metabolic energy sources available for the development of life, possibly resembling life as we know it (Westall et al., 2013; Grotzinger et al., 2014; Kral et al., 2014; Hurowitz et al., 2017). Traces of this life may have been entombed in rocks, and because Mars lacks global plate tectonics, most ancient rocks have stayed at the surface without undergoing metamorphism, unlike the ancient rocks on Earth. Space agencies worldwide are thus sending rovers to Mars to search for ancient biosignatures in the ancient Martian geological record, anticipating their identification directly *in situ* or, more likely, within samples which will have returned to Earth (Goetz et al., 2016; Vago et al., 2017; Farley et al., 2020; Bosak et al., 2021).

Ancient Martian terrains (> 3.7 Ga) covered by clay minerals are the main targets for the astrobiological exploration of Mars (Pajola et al., 2017; Salvatore et al., 2018; Quantin-Nataf et al., 2021). In addition to being at the heart of the "clay life" hypothesis, which posits that life began as self-replicating minerals (Cairns-Smith, 1966; Joshi et al., 2015; Brucato and Fornaro, 2019), clay minerals have strong absorption capacities, conferring them a high 'potential of biopreservation' (Hedges and Keil, 1995; Kennedy et al., 2002; Ehlmann et al., 2008; Westall and Cockell, 2016). The presence of these minerals at landing sites of robotic missions is thus believed to maximize the chances of detecting diagnostic organic molecules, thereby eventually evidencing the past existence of Martian Life (Summons et al., 2008, 2011; McMahon et al., 2018; Bosak et al., 2021). Odds to find traces of life in ancient Martian rocks rich in clay minerals are seen as very high given that the loss of the atmosphere during the Hesperian (3.7 to 3.2 Ga) and the Amazonian (3.2 Ga to present) resulted in a drastic decrease of surface temperatures, transmuting Mars subsurface into a giant freezer (Clifford et al., 2010).

However, the subsurface of Mars may not be that suitable for the preservation of organic biosignatures. In addition to the detrimental effect of the pervasive presence of highly oxidizing Cl-rich species such as perchlorates (Hecht et al., 2009; Quinn et al., 2013; Leshin et al., 2013; Lasne et al., 2016), orbital and in-situ exploration have revealed that most Noachian clay-rich sediments are intruded by veins of (Ca, Fe, Mg, Al)-sulfates, attesting to the episodic circulation of (more or less acidic) brines at low to relatively high temperatures (Zolotov and Mironenko, 2016; Schwenzer et al., 2016; Kronyak et al., 2019; Bristow et al., 2021). Such fluid circulation events may have been triggered by volcanism or impacts. In fact, any impactor, even a small one, will deliver enough energy to melt and mobilize the water ice trapped in the Martian subsurface (Boynton et al., 2002; Bramson et al., 2015; Dundas et al., 2018; Piqueux et al., 2019), initiating a long lasting circulation of fluids over distances possibly considerable (i.e.

several hundreds of kilometers - Rathbun and Squyres, 2002; Segura et al., 2002; Barnhart et al., 2010; Ivanov and Pierazzo, 2011; Osinski et al., 2013). Because liquid water enhances the reactivity of organic compounds (McCollom et al., 2001; Lewan and Roy, 2011; Foustoukos and Stern, 2012), such episodes of fluid circulation can only be detrimental to the preservation of organic biosignatures, thus complicating their recognition. To date, we do not know which (nor in what state) organic biosignatures can be preserved within clay-rich Martian rocks.

A few experimental studies have dealt with the preservation/degradation of organic-clay mixtures under simulated hydrothermal Martian conditions. Yet, these hydrous pyrolysis experiments have been conducted either using single molecules, such as RNA (Viennet et al., 2019) or glycine (Dalai et al., 2017; Gil-Lozano et al., 2020), or using complex natural samples (Tan et al., 2021), rather than using model microorganisms experimentally mixed within a pure synthetic mineral matrix, as previously done by some authors to document the effect of diagenesis under terrestrial conditions (Oehler and Schopf, 1971; Li et al., 2014; Picard et al., 2015; Alleon et al., 2016; Miot et al., 2017; Igisu et al., 2018). Here, we report results of laboratory experiments conducted using cells of a model microorganism (i.e., *Escherichia coli* cells) and pure saponite (a Mg-rich trioctahedral smectite) synthesized in the lab. We exposed mixtures of *E. coli* cells and saponite to thermal treatments under a Martian atmosphere (CO_2) in the presence of water, thereby simulating episodes of fluid circulation. Of note, rather than exactly replicating the processes that may have taken place on Mars, the present experiments have been designed to constrain the impact of temperature conditions on the chemical degradation of microbial signatures in the presence of clay minerals and water, thereby providing information on what can be found (and thus pinpointing what should be searched for) in the ancient Martian geological record. Here, we used elemental analyses, infrared (IR) spectroscopy and X-ray diffraction (XRD) to document the chemistry of the organic materials composing the residues as well as the nature and crystallinity of the associated mineral assemblage. The presence of organic compounds within the interlayer spaces of clays is discussed based on additional XRD measurements conducted under vacuum.

2. MATERIALS & METHODS

2.1. Starting Materials

2.1.1. Escherichia coli

Although extremophilic microorganisms are often used in astrobiological studies dealing with survivability, *Escherichia coli* was chosen as a model microorganism for the experiments reported here because it is a simple, well-known bacterium, used as a model microorganism in many biological studies (Taj et al., 2014; Blount, 2015; Samie, 2017; Ruiz and Silhavy, 2022). *E. coli* cells were grown at IMPMC in Paris: 10 mL suspension of precultured *E. coli* cells (C41 ccya B strain) was transferred into 1 liter of LB Lennox broth medium (20 g/L) (Sigma-Aldrich) containing kanamycin (30 $\mu g.mL^{-1}$) to prevent growth of potential contaminants. Cells were allowed to multiply overnight before being harvested by centrifugation 4 times at 5000 rpm during 30 min and rinsed with distilled water at 6500 rpm for 10 min. Cells were then dried overnight at 50°C.

2.1.2. Saponite synthesis

Martian orbital and *in situ* observations have revealed that clay minerals are widespread in Noachian terrains (*i.e*. terrains older than 3.7 Ga). Among these minerals, smectites with compositions ranging from nontronite (Fe) to saponite (Mg) are the most abundant (Ehlmann et al., 2011; Carter et al., 2013). In order to investigate the biopreservation potential of smectites on Mars while avoiding the potential additional effect of iron, we have chosen a Mg-rich smectite (*i.e*. a saponite) to conduct our experiments. This smectite was synthesized in the lab following the protocol described in Criouet et al. (in press): diluted solutions (0.2M) of Na_2SiO_3 $5H_2O$ (Sigma Aldrich, >95%), $AlCl_3$ $6H_2O$ (Sigma Aldrich, 99%), $MgCl_2$ $6H_2O$ (Sigma Aldrich, >99%) were mixed to produce a gel stoichiometrically identical to a pure saponite of composition $Na_{0.4}(Si_{3.6}Al_{0.4})Mg_3O_{10}(OH)_2$. The gel was then immersed into pure water (milliQ – 18.2 MΩ.cm) in a PTFE reactor for crystallization at 230 °C (~28 bars) for 10 days. The produced saponite was then filtered and dried at 50°C for 24h.

2.2. Experimental procedure

Mixtures of 100 mg of dried synthetic saponite and 42 mg of dried *E. coli* cells (*i.e*. corresponding to a total of 15 wt.% of carbon in the starting material) were loaded into Ti-reactors (Fig. S1) in which was added 1 mL of milliQ water (18.2 MΩ-cm) for a water-to-rock ratio (W:R) of 7:1. Because the gas phase (*i.e*. the atmosphere) can strongly influence the final organo-mineral assemblages (Schiffbauer et al., 2012; Viennet et al., 2020), reactors were closed under a pure CO_2 atmosphere (1 bar) before being placed into ovens for the experiments. A first series of experiments was conducted at 100, 150 and 200 °C for 10 days, and a second series of experiments was conducted at 150°C for 1, 10 and 100 days. Duplicate experiments were conducted at 150°C for 10 days to ensure reproducibility. Control experiments were conducted at the same temperatures (100, 150 and 200°C) and for the same durations (1, 10 and 100 days) with only saponite (*i.e.* in the absence of *E. coli* cells) and with only *E. coli* cells (*i.e.* in the absence of saponite). At the end of the experiments, the water-soluble fractions were extracted from the solid residues by rinsing and centrifuging until the water was clear. Only the solid residues were analyzed, after being dried at 50°C overnight. Residues of experiments conducted at 150°C for different durations were also dried on glass slides, at room temperature, to obtain oriented preparations for XRD.

2.3. Characterization techniques

The total organic carbon (TOC) and total nitrogen (TN) contents as well as the carbon isotope composition ($\delta^{13}C$) of the residues were measured using a Flash 2000 Thermo CHNSO elemental analyzer (EA) coupled to a Thermo Scientific DeltaV Advantage irMS operated at the SSMIM facility at MNHN in Paris. A mass of 1.2 mg of each residue was loaded in Sn capsules and combusted under oxygen/helium flux at 1020°C. The N_2 and CO_2 released by combustion were separated by a chromatography column and quantified using a thermal conductivity detector. The calibration was performed with about 0.3 mg of 4 to 9 alanine

standards. Mid-infrared (Mid-IR) reflectance spectroscopy measurements were conducted using a Fourier transform spectrometer Nicolet 6700 FTIR operating at IMPMC (Paris, France) equipped with a KBr beamsplitter and a DTGS KBr detector. Spectra were collected over the 400-4000 cm^{-1} range with a 4 cm^{-1} resolution in attenuated total reflection mode (ATR) using a Specac Quest ATR device fitted with a diamond internal reflection element. The X-ray diffraction (XRD) patterns were collected on powder (placed on Si zero diffraction plates) at room temperature, with a step size of 0.033°2θ over the 3–75 °2θ Cok$\alpha_{1,2}$ angular range with a counting time of 300 ms per step, using an X'Pert Pro instrument from PANalytical, equipped with a cobalt source (Cokα 40 mA) and operating at IMPMC (Paris, France). The XRD patterns of the residues of experiments conducted at 150°C for different durations were also measured on oriented preparations, at room temperature, using the same instrument, over the 4–12 °2θ Cok$\alpha_{1,2}$ angular range (step size of 0.033°2θ, counting time of 300 ms per step), at both atmospheric pressure and under vacuum (3.10^{-4} atmosphere) using an Anton Parr HTK 1200 oven coupled to an EDWARDS RV3 pump, in order to determine if organic molecules were trapped within the interlayer spaces of the smectites.

3. RESULTS

3.1. EA-irMS (Elemental Analysis and isotope ratio Mass Spectrometry)

Control experiments conducted in the absence of saponite (*i.e.* with only *E. coli* cells) reveal that the TOC (total organic carbon) of the residues has increased with increasing temperature and with increasing duration at 150°C (Table 1, Fig. 1): from about 45 wt. % for the pristine *E. coli* cells to almost 70 wt. % for the residues of the experiments conducted at 200°C for 10 days and at 150°C for 100 days. In contrast, the TN (total nitrogen) content of the residues has decreased, leading to a net decrease of the atomic N/C ratio. Last, $\delta^{13}C$ values have decreased with increasing temperature and duration (the residues are richer in ^{12}C than the starting material - cf Table 1).

Things are different for residues of experiments conducted in the presence of saponite. In fact, instead of having increased, the TOC of the residues has decreased with increasing temperature and with increasing duration at 150°C, dropping from about 14 wt. % for the pristine mixture of E. coli cells and saponite to less than 6 wt. % for the residues from experiments conducted at 150°C for 10 and 100 days (Table 1, Fig.1). Similarly, the TN (total nitrogen) content of the residues has decreased. However, the N/C atomic ratio has not drastically changed during the experiments, as is the case for the carbon isotope composition, which remains rather similar to that of the starting material. Of note, the fact that the experiment conducted at 200°C for 10 days exhibits a higher TOC than those conducted at 150°C for 10 days could be due to the insolubilization of organic molecules present in the soluble fraction at lower temperatures (i.e. < 200°C)

3.2. Mid-IR (Mid-infrared spectroscopy)

Pristine *E. coli* cells exhibit a Mid-IR spectrum very similar to the spectra of bacteria reported in the literature (Fig. 2 – Legal et al., 1991; Nadtochenko et al., 2005; Erukhimovitch et al., 2005; Garip et al., 2007; Filip et al., 2008; Nyarko et al., 2014; Li et al., 2014; Faghihzadeh et al., 2016). The four major peaks at 1651-1626, 1528, and 1515 cm^{-1} can be attributed to amide I ($\nu C=O$), amide II ($\delta N-H$ and $\nu C-N$) and aromatic bands of proteins, respectively. Noticeably, features at 1468 and 1451 cm^{-1} corresponding to C-H deformations (or $R-NH_3^+$ for the band at ~1450 cm^{-1} – Viennet et al., 2022) and at ~1395 cm^{-1} corresponding to $\nu_s C=O$ vibrations (Erukhimovitch et al., 2005; Garip et al., 2007; Faghihzadeh et al., 2016) or C-H bending / νCH_3 in fatty acids (Filip et al., 2008; Li et al., 2014) also exist in this spectral region (Legal et al., 1991). The band at 1227 cm^{-1} may be attributed to $\nu_{as} P=O$ (Legal et al., 1991; Garip et al., 2007) or amide III vibrations (Filip et al., 2008; Li et al., 2014), while bands at 1170, 1153 and 1118 cm^{-1} correspond to $\nu C-O$, or $\nu C-N$ vibrations. In addition, the broad band near 1060 cm^{-1} may result from the overlap of several bands corresponding to carbohydrates (Legal et al., 1991; Nadtochenko et al., 2005; Erukhimovitch et al., 2005; Nyarko et al., 2014). Bands at 2958, 2923, 2873 and 2853 cm^{-1} are related to νCH_3 and νCH_2 vibrations, and bands at 3277 cm^{-1} and 3067 cm^{-1} correspond to $\nu N-H$ vibrations (Legal et al., 1991; Filip et al., 2008; Faghihzadeh et al., 2016). Of note, δOH vibrations from water may also contribute to the absorption band at about 1630 cm^{-1}.

In the absence of saponite, the IR spectral signature of *E. coli* cells has gradually changed with increasing temperature and experimental duration, with a strong decrease of intensity of most of the main bands corresponding to C-N, C-O and P=O bonds (i.e., bands in the 1300-600 cm^{-1} range – Fig. 2). Absent from the spectrum of the pristine *E.coli* cells, an additional band at 1695 cm^{-1} (attributed to $\nu C=O$ vibrations) is observed in the spectra of residues produced at 150°C and above, which may indicate a degradation of the cellular membrane (Faghihzadeh et al., 2016). The increase of this band with increasing temperature and experimental duration is concomitant to a decrease of the shoulder at 1651 cm^{-1}. Besides C-H bands, most of the bands present in the spectrum of the pristine *E. coli* cells are less intense in the spectra of residues, including the band corresponding to OH groups. Bands at 1227 and 1118 cm^{-1} are no longer present in the spectrum of the residue of the experiment conducted at 200°C, and those corresponding to $\nu N-H$, $\nu C=O$, amide I and amide II are respectively shifted to 3324, 3060, 1700, 1636 and 1538 cm^{-1}.

The presence of saponite modifies the IR signal of the starting material, with saponite peaks dominating the 400-1200 cm^{-1} and the 3000-4000 cm^{-1} spectral regions (Fig. 3 & S2). Bands corresponding to *E. coli* cells are similar in the 1200-1800 cm^{-1} and 2800-4000 cm^{-1} spectral regions, but the bands near 1530 cm^{-1} (amides II), 1515 cm^{-1} (aromatic $\nu C=C$), 1468 cm^{-1} (C-H), 1450 cm^{-1} (C-H or $R-NH_3^+$), 1405 / 1390 cm^{-1} ($\nu C=O$ symmetric vibrations of COO^- group or C-H) and 1227 cm^{-1} (amide III or $\nu_{as} P=O$) are less intense. Besides C-H bands (at 2800-3000 cm^{-1} and at 1470-1456 cm^{-1}), the intensity of most bands decreases with increasing temperature and experimental duration, in a more drastic way than in the absence of saponite. For instance, the band attributed to amide III or phosphate groups (at 1227 cm^{-1}) is no longer present in the

spectra of the residues of experiments conducted above 100°C, while it is still present in the spectra of residues of experiments conducted at 150°C in the absence of saponite. As in the absence of saponite, the intensity of the band near 1650 cm^{-1} decreases with increasing temperature and experimental duration, and its position has shifted to 1628 cm^{-1} after 10 days at 150°C. A shoulder at 1695 cm^{-1}, attributed to νC=O, is observed in most residues of experiments conducted in the presence of saponite. As in the absence of saponite, besides C-H bands, weak bands are still present near 3277, 3067, 1695, 1633, 1564, 1515 and 1378 cm^{-1} in the spectrum of the residue of the experiments conducted at 200°C, and a band corresponding to amide I (at 1628 cm^{-1}) can still be observed in the spectrum of the residue of the experiments conducted at 150°C for 100 days. Of note, the band at 530 cm^{-1} corresponding to Si-O-Mg vibrations (Madejová et al., 2017; Besselink et al., 2020; J. T. Kloprogge and Ponce, 2021) is no longer present in the spectra of the residues of experiments (Fig. 3), while the band at 750 cm^{-1}, absent in the spectrum of the starting material, possibly corresponds to Si-O-^{IV}Al vibrations (Madejová et al., 2017), Al-OH vibrations (Kloprogge and Frost, 2000) or Mg_2-Al-OH deformations (Kloprogge and Ponce, 2021). This band is also present in the spectra of the control experiments conducted in the absence of *E. coli* cells (see Fig. S2).

3.3. XRD

The XRD patterns of the residues of experiments conducted in the absence of *E. coli* cells reveal that saponite is stable at all the temperatures investigated (*i.e.*, saponite is the only crystalline phase – Fig. S2), with a (001) reflection indicating an interlayer space of about 12 to 12.6 Å. Of note, a slight effect of recrystallization may have occurred for the experiments conducted at 150°C for 100 days and at 200°C for 10 days, as suggested by the shift of their 02.11 and 06.33 reflections from 4.54 to 4.55 Å and from 1.525 to 1.526 Å, respectively (Fig. S2), but these shifts may be due to slight variations in hydration. The same is true in the presence of *E. coli* cells (Fig. 4). The 02.11 and 06.33 reflections are shifted from 4.55 to 4.56 Å and 1.526 to 1.527 Å, but the position of the (001) reflection indicates an interlayer space of about 13.5-15 Å (*vs.* 12-12.6 Å for the experiments conducted without *E. coli* cells), either due to mixed-layer stacking and/or trapping of organic compounds (Viennet et al., 2019, 2020, 2022).

Under vacuum, the interlayer space of the saponite of the residues produced in the presence of *E. coli* cells does not collapse, as indicated by the absence of shift of the 001 reflection in the XRD patterns, in contrast to that of the pristine crystalline saponite never exposed to *E. coli* cells which collapses from 12 to 10.45 Å (Fig. 5). This attests to the presence of organic compounds locking the interlayer spaces of saponite (Viennet et al., 2019, 2020, 2022). Of note, the interlayer space of the saponite in the residues produced at 150°C in the presence of *E. coli* cells decreases as the experimental duration increases (from 1 to 100 days – Fig. 5), suggesting a reduction of the amount and/or the size of the organic compounds trapped within interlayer spaces (Lanson et al., 2022). This trend is consistent with EA-irMS results, indicating a decreasing TOC and TN content with increasing experimental duration (Table 1, Fig. 1).

4. DISCUSSION

Temperature has a significant detrimental effect on microbial signatures, as shown by the results of the control experiments conducted here with *E. coli* cells (*i.e.* in the absence of saponite), confirming previous results reported in the literature (Oehler and Schopf, 1971; Li et al., 2014; Picard et al., 2015; Alleon et al., 2016; Miot et al., 2017; Igisu et al., 2018). The increase of temperature conditions leads to significant denitrification, deoxygenation and dehydrogenation, thereby producing residues exhibiting high TOC, low N/C ratio and spectral signatures drastically different from that of the starting material (Table 1, Fig. 1 & 2). At 150°C, the N/C ratio of the residues of the control experiments conducted with *E. coli* cells (*i.e.* in the absence of saponite) exhibits a log-linear relationship with experimental duration (Fig. 1). Such behavior cannot be related to any reaction mechanism commonly operating in solid/solid organic reactions (Rothenberg et al., 2001). However, similar log-linear behaviors have been reported for parameters describing the maturation/degradation of carbon materials as a function of the duration of thermal treatments. This suggests that the degradation of *E. coli* cells mainly occurs through a series of kinetically controlled reactions such as chain scissions coupled to polymerization/condensation reactions (Rothenberg et al., 2001; Vandenbroucke and Largeau, 2007; Sánchez-Jiménez et al., 2010; Pérez-Maqueda et al., 2014). The results of the present experiments suggest that a likely metastable equilibrium is achieved in only a few days (no significant evolution of the N/C ratio occurs between 10 and 100 days), which is consistent with previous experimental results (Alleon et al., 2016, 2017). Presumably, this equilibrium could last for much longer durations, suggesting that no significant additional chemical degradation would occur during geological times if conditions remain the same, *i.e.* in the absence of mineral phases.

Obviously, experiments investigating the degradation/preservation of traces of life have to be conducted in the presence of mineral phases to provide information about processes occurring in natural settings. As an expandable clay mineral, saponite is believed to have a high potential for biopreservation (Hedges and Keil, 1995; Kennedy et al., 2002; Ehlmann et al., 2008; Westall and Cockell, 2016). In fact, in addition to adsorption/complexation of organic compounds at edge sites (Kleber et al., 2021), clay minerals may trap organic compounds within their interlayer spaces (Laird et al., 1989; Johnston et al., 2001; Viennet et al., 2019, 2022). Interlayer water molecules of smectites can be replaced by a variety of neutral organic molecules, such as carbohydrates or hydroxyl compounds, but the intercalation of protonated species (i.e., cationized organic molecules) via H_2O bridges or cation exchange is much more effective (Lagaly, 1984; Lagaly et al., 2006). Organic cations may even intercalate beyond the cation exchange capacity if van der Waals forces play a major role in binding molecules to surfaces (Lagaly et al., 2006; Bergaya and Lagaly, 2011). Trapping of organic compounds by smectites has been previously reported in natural systems as well as in laboratory experiments (Aufdenkampe et al., 2001; Kopittke et al., 2018; Viennet et al., 2019, 2020). Consistently, the present experiments evidence that clay minerals have adsorbed/trapped organic compounds within their interlayer spaces as indicated by XRD (Fig. 4 & 5), thereby delaying their chemical degradation. Here, the evolution of the N/C ratio of the experimental residues pinpoints a preferential trapping of N-rich compounds by saponite. In fact, except for the experiments

conducted at 200°C and at 150°C for 100 days, the N/C ratio of the residues of experiments conducted in the presence of saponite and *E. coli* cells are higher than those of pristine *E. coli* cells (Table 1). Such a preferential trapping may be explained by the fact that smectites are more likely to trap N-rich organic molecules as they are more readily cationized (e.g., protonated) than N-poor compounds (e.g., van Santen and Liu, 2018; Kleber et al., 2021).

The preferential trapping of N-rich compounds may also explain the evolution of the $\delta^{13}C$ values with increasing time and temperature (Table 1). Indeed, the different biochemical components of living organisms have different carbon isotopic composition (Galimov, 2012), the $\delta^{13}C$ values of nucleic acids having roughly the same $\delta^{13}C$ values as the cells, while proteins are slightly depleted in ^{13}C, lipids even more depleted, and carbohydrates slightly enriched in ^{13}C (Spiker and Hatcher, 1984; Blair et al., 1985; Hayes, 2001; Galimov, 2012). In the absence of saponite, the degradation of *E. coli* cells with increasing temperature or experimental duration leads to a relative enrichment in lipids (which degrade at higher temperature than the other components - Chen et al., 2005), resulting in a decrease of the $\delta^{13}C$ values of the residues. In the presence of saponite, the preferential trapping of N-rich compounds (i.e. proteins or nucleic acids) limits this decrease since the compounds trapped within their interlayer spaces of smectites are initially richer in ^{13}C than lipids (Macko et al., 1987; Galimov, 2012).

However, such trapping of organic compounds does not completely preserve them from degradation with increasing temperature and experimental duration, as shown by the N/C and $\delta^{13}C$ values, Mid-IR spectra and XRD patterns of the residues of experiments conducted at 200°C or at 150°C for 100 days (Table 1, Fig. 1, 2 & 5). This suggests that saponite is not that efficient in protecting biogenic organic compounds from thermal degradation over long periods of time, in contrast to silica (Alleon et al., 2016; Igisu et al., 2018) or biominerals such as Ca-phosphates (Li et al., 2014) or Fe-oxyhydroxides (Picard et al., 2015). Plus, smectites have long been known to promote organic compound maturation and thermal cracking (e.g., Johns, 1979; Horsfield and Douglas, 1980; Goldstein, 1983; Espitalié et al., 1984; Nikalje et al., 2000; Rahman et al., 2018). The effectiveness of smectites in promoting organic reactions involved in hydrocarbon generation has been demonstrated in many experimental studies: Lewis-acid sites, characterized by Al^{3+} or Fe^{3+} at the edges of smectites, and Brønsted-acid sites, located in the interlayer spaces, are effective in promoting decarboxylation and hydrocarbons cracking (Yuan et al., 2013; Bu et al., 2017; Du et al., 2021; Cai et al., 2022). Although saponite is less efficient than montmorillonite in promoting such organic reactions (Eberl et al., 1978; Whitney, 1983; Pusch and Karnland, 1988), its high Mg content may be detrimental to the preservation of organic compounds. In fact, although life requires divalent cations (Adamala et al., 2016; Dalai et al., 2018), relatively low concentrations of Mg^{2+} will disrupt vesicles made of fatty acids by promoting their precipitation (Monnard et al., 2002; Deamer, 2017; Dalai et al., 2018; Hong et al., 2018), and the membrane of *E.coli* cells exhibits a rather high concentration of fatty acids (Lugtenberg, 1981; Nikaido, 2003; Sohlenkamp and Geiger, 2016; Wang et al., 2021). In any case, in contrast to the general belief, the present experiments demonstrate that saponite may not have a high potential for chemical biopreservation.

The present results have strong implications for the search for traces of life in the ancient clay-rich rocks lying at the surface of Mars. Determining what could be found in Martian rocks is critical for the ongoing astrobiological exploration of Mars (Summons et al., 2011; Westall et al., 2015; Hays et al., 2017; McMahon et al., 2018; Bosak et al., 2021). To date, a number of studies have experimentally investigated the thermal degradation of microorganisms in the presence of various mineral phases (Oehler and Schopf, 1971; Li et al., 2014; Picard et al., 2015; Alleon et al., 2016; Miot et al., 2017; Igisu et al., 2018), while some have investigated the influence of the presence of clay minerals on the thermal degradation of specific organic compounds (Viennet et al., 2019, 2020, 2022; Jacquemot et al., 2019; Vinogradoff et al., 2020a, 2020b), but none have investigated what would become a mixture of smectites and microbial cells during an episode of fluid circulation under (rather realistic) Martian conditions as done in the present study.

In contrast to the general belief, the present study illustrates that we should not expect to detect pristine biogenic organic compounds on Mars, but rather by-products of their degradation. Although $\delta^{13}C$ values can be preserved to some extent, depending on the temperature and the duration of the experiments, it remains of limited interest for the search for traces of life on Mars given that a number of abiotic pathways may lead to the production of organic compounds exhibiting $\delta^{13}C$ values similar to "typical biogenic" values (Craig, 1954; Horita, 2005; McCollom and Seewald, 2006). Plus, as on Earth, the $\delta^{13}C$ values of Martian microbial organic compounds would depend on the values of the carbon sources and on the pathways of production, i.e. on metabolisms (Hayes, 1993; Zhang, 2002; Adrian and Marco-Urrea, 2016), both remaining to be identified. Still, the present experiments demonstrate that smectites selectively and efficiently trap N-rich organic compounds within their interlayer spaces. Although thermal degradation processes may significantly alter their initial chemical and molecular structure, the remaining N-rich compounds may be considered as molecular fossils to search for in the ancient Martian geological record.

Obviously, the presence of N-rich organic materials within smectites should not be the only 'biosignature' to consider when searching for traces of life in Martian rocks: some information may also be derived from the mineral assemblage itself, as previously suggested (Viennet et al., 2019; Jacquemot et al., 2019). For instance, a quite uncommon mineral assemblage comprising clay-organic complexes intimately associated with (poorly crystallized) nanoscale phosphates and carbonates could possibly be used to attest to the past presence of microbial life (Viennet et al., 2019; Jacquemot et al., 2019). Determining if such an assemblage is present in the experimental residues of the present study would require characterizing them using a combination of the most advanced microscopic and spectroscopic tools available in laboratories worldwide, as it will be the case for the future samples which will be returned from Mars. In the same way, additional characterization of experimental residues could be carried out using advanced mass spectrometric techniques, such as gas or liquid chromatography (GC or LC), matrix-assisted laser desorption/ionization (MALDI) or Fourier-transform ion cyclotron resonance (FT-ICR) coupled to high resolution mass spectroscopy, to document the diversity of organic molecules in presence after a simulated episode of fluid circulation.

Altogether, the present work can be seen as a first step towards a better understanding of the taphonomic processes having possibly impacted Martian fossil biosignatures, but going further will require additional experiments. Here, we used *E. coli* as a model microorganism, but similar experiments should be conducted with other microorganisms exhibiting different protein/lipid/sugar ratios. Also, we conducted experiments with Mg-smectites, but smectites containing other cations, such as Al or Fe, may exert a different influence on the thermal degradation of organic compounds. Although the effect of octahedrally charged smectites (i.e. montmorillonites) is already well known (Yuan et al., 2013; Bu et al., 2017; Du et al., 2021; Cai et al., 2022), the one of tetrahedrally charged dioctahedral Fe and Al-rich smectites (i.e. nontronites, beidellites) remains to be determined. In the same way, because the fluids penetrating the clay-rich units on Mars are likely to be richer in sulfates than pure water, additional experiments should be conducted with fluids exhibiting variable concentrations in sulfates, the chemistry of the fluid being likely to control organic reactions and interactions with clay minerals. Finally, fluid-flow experiments, i.e. experiments under open system conditions, should also be conducted, since natural settings are rarely behaving as closed systems. Although a lot has still to be achieved, there is no doubt that laboratory experiments will contribute to the development of a robust framework to support the ongoing astrobiological exploration of Mars and the future astrobiological exploration of the Solar System.

ACKNOWLEDGMENTS

The authors wish to acknowledge the spectroscopic and X-ray diffraction facilities of IMPMC and Elisabeth Malassis for administrative support. This work was made possible thanks to financial support from the ATM program at MNHN (Project BioMars - PI: S. Bernard), from the Institut des Matériaux of Sorbonne Université (IMat) (Project Ageing on Mars - PI: S. Bernard) and from the European Research Council (ERC Consolidator Grant No. 819587: HYDROMA - PI: L. Remusat). The authors declare that they have no known competing financial interests or personal relationships that could have appeared to influence the work reported in this article.

DATA AVAILABILITY

All data are available at https://drive.google.com/drive/folders/1P903A46df6onvXIUtSz8ECWb9XU7vDuK?usp=drive_link

AUTHORS' CONTRIBUTION

IC, JCV and SB designed the present study. FSP cultured *E. coli*. IC conducted the syntheses of saponite and the fossilization experiments. IC and JCV performed the FTIR and the XRD analyses, with the help of LD and MG. All authors contributed to the interpretation of the data and discussed their implications. IC, JCV and SB wrote the present manuscript, with critical inputs from EB, AB, FB and LR.

APPENDIX A. SUPPLEMENTARY MATERIAL

Figure S1. Picture of the reactors used for the experiments.

Figure S2. Mid-IR spectra and XRD patterns of the saponite starting material (in grey) and the residues of control experiments conducted in the absence of E. coli cells (i.e., pure saponite at 150°C for 100 days (in brown), and pure saponite at 200°C for 10 days (in dark grey)).

REFERENCES

Adamala K. P., Engelhart A. E. and Szostak J. W. (2016) Collaboration between primitive cell membranes and soluble catalysts. *Nat Commun* **7**, 11041.

Adrian L. and Marco-Urrea E. (2016) Isotopes in geobiochemistry: tracing metabolic pathways in microorganisms of environmental relevance with stable isotopes. *Current Opinion in Biotechnology* **41**, 19–25.

Alleon J., Bernard S., Le Guillou C., Daval D., Skouri-Panet F., Kuga M. and Robert F. (2017) Organic molecular heterogeneities can withstand diagenesis. *Sci Rep* **7**, 1508.

Alleon J., Bernard S., Le Guillou C., Daval D., Skouri-Panet F., Pont S., Delbes L. and Robert F. (2016) Early entombment within silica minimizes the molecular degradation of microorganisms during advanced diagenesis. *Chemical Geology* **437**, 98–108.

Aufdenkampe A. K., Hedges J. I., Richey J. E., Krusche A. V. and Llerena C. A. (2001) Sorptive fractionation of dissolved organic nitrogen and amino acids onto fine sediments within the Amazon Basin. *Limnology and Oceanography* **46**, 1921–1935.

Barnhart C. J., Nimmo F. and Travis B. J. (2010) Martian post-impact hydrothermal systems incorporating freezing. *Icarus* **208**, 101–117.

Bergaya F. and Lagaly G. (2011) Intercalation processes of layered minerals. In *Layered Mineral Structures and their Application in Advanced Technologies* (eds. M. F. Brigatti and A. Mottana). Mineralogical Society of Great Britain and Ireland. p. 0.

Besselink R., Stawski T. M., Freeman H. M., Hövelmann J. and To D. J. (2020) Mechanism of saponite crystallization from a rapidly formed amorphous intermediate. , 32.

Bianciardi G., Miller J. D., Straat P. A. and Levin G. V. (2012) Complexity analysis of the Viking Labeled Release experiments. *International Journal of Aeronautical and Space Sciences* **13**, 14–26.

Blair N., Leu A., Muñoz E., Olsen J., Kwong E. and Des Marais D. (1985) Carbon isotopic fractionation in heterotrophic microbial metabolism. *Appl Environ Microbiol* **50**, 996–1001.

Blount Z. D. (2015) The unexhausted potential of E. coli. *eLife* **4**, e05826.

Bosak T., Moore K. R., Gong J. and Grotzinger J. P. (2021) Searching for biosignatures in sedimentary rocks from early Earth and Mars. *Nat Rev Earth Environ* **2**, 490–506.

Boynton W. V., Feldman W. C., Squyres S. W., Prettyman T. H., Bruckner J., Evans L. G., Reedy R. C., Starr R., Arnold J. R., Drake D. M., Englert P. a. J., Metzger A. E., Mitrofanov I., Trombka J. I., D'Uston C., Wanke H., Gasnault O., Hamara D. K., Janes D. M., Marcialis R. L., Maurice S., Mikheeva I., Taylor G. J., Tokar R. and Shinohara C. (2002) Distribution of hydrogen in the near surface of Mars: evidence for subsurface ice deposits. *Science* **297**, 81–85.

Bramson A. M., Byrne S., Putzig N. E., Sutton S., Plaut J. J., Brothers T. C. and Holt J. W. (2015) Widespread excess ice in Arcadia Planitia, Mars. *Geophysical Research Letters* **42**, 6566–6574.

Bristow T. F., Grotzinger J. P., Rampe E. B., Cuadros J., Chipera S. J., Downs G. W., Fedo C. M., Frydenvang J., McAdam A. C., Morris R. V., Achilles C. N., Blake D. F., Castle N., Craig P., Des Marais D. J., Downs R. T., Hazen R. M., Ming D. W., Morrison S. M., Thorpe M. T., Treiman A. H., Tu V., Vaniman D. T., Yen A. S., Gellert R., Mahaffy P. R., Wiens R. C., Bryk A. B., Bennett K. A., Fox V. K., Millken R. E., Fraeman A. A. and Vasavada A. R. (2021) Brine-driven destruction of clay minerals in Gale crater, Mars. *Science* **373**, 198–204.

Broz A. P. (2020) Organic matter preservation in ancient soils of Earth and Mars. *Life (Basel)* **10**, 113.

Brucato J. R. and Fornaro T. (2019) Role of Mineral Surfaces in Prebiotic Processes and Space-Like Conditions. In *Biosignatures for Astrobiology* (eds. B. Cavalazzi and F. Westall). Advances in astrobiology and biogeophysics. Springer International Publishing, Cham. pp. 183–204.

Bu H., Yuan P., Liu H., Liu D., Liu J., He H., Zhou J., Song H. and Li Z. (2017) Effects of complexation between organic matter (OM) and clay mineral on OM pyrolysis. *Geochimica et Cosmochimica Acta* **212**, 1–15.

Cai J., Du J., Song M., Lei T., Wang X. and Li Y. (2022) Control of clay mineral properties on hydrocarbon generation of organo-clay complexes: evidence from high-temperature pyrolysis experiments. *Applied Clay Science* **216**, 106368.

Cairns-Smith A. G. (1966) The origin of Life and the nature of the primitive gene. *Journal of Theoretical Biology* **10**, 53–88.

Carter J., Poulet F., Bibring J.-P., Mangold N. and Murchie S. (2013) Hydrous minerals on Mars as seen by the CRISM and OMEGA imaging spectrometers: updated global view. *J. Geophys. Res. Planets* **118**, 831–858.

Chen I. A., Salehi-Ashtiani K. and Szostak J. W. (2005) RNA catalysis in model protocell vesicles. *J. Am. Chem. Soc.* **127**, 13213–13219.

Clifford S. M., Lasue J., Heggy E., Boisson J., McGovern P. and Max M. D. (2010) Depth of the Martian cryosphere: revised estimates and implications for the existence and detection of subpermafrost groundwater. *Journal of Geophysical Research: Planets* **115**.

Craig H. (1954) Geochemical implications of the isotopic composition of carbon in ancient rocks. *Geochimica et Cosmochimica Acta* **6**, 186–196.

559 Dalai P., Pleyer H. L., Strasdeit H. and Fox S. (2017) The influence of mineral matrices on the
560 thermal behavior of glycine. *Orig Life Evol Biosph* **47**, 427–452.

561 Dalai P., Ustriyana P. and Sahai N. (2018) Aqueous magnesium as an environmental selection
562 pressure in the evolution of phospholipid membranes on early earth. *Geochimica et*
563 *Cosmochimica Acta* **223**, 216–228.

564 Deamer D. (2017) The role of lipid membranes in Life's origin. *Life* **7**, 5.

565 Du J., Cai J., Lei T. and Li Y. (2021) Diversified roles of mineral transformation in controlling
566 hydrocarbon generation process, mechanism, and pattern. *Geoscience Frontiers* **12**,
567 725–736.

568 Dundas C. M., Bramson A. M., Ojha L., Wray J. J., Mellon M. T., Byrne S., McEwen A. S.,
569 Putzig N. E., Viola D., Sutton S., Clark E. and Holt J. W. (2018) Exposed subsurface
570 ice sheets in the Martian mid-latitudes. *Science* **359**, 199–201.

571 Eberl D., Whitney G. and Khoury H. (1978) Hydrothermal reactivity of smectite. *American*
572 *Mineralogist* **63**, 401–409.

573 Ehlmann B. L., Mustard J. F., Fassett C. I., Schon S. C., Head III J. W., Des Marais D. J., Grant
574 J. A. and Murchie S. L. (2008) Clay minerals in delta deposits and organic preservation
575 potential on Mars. *Nature Geosci* **1**, 355–358.

576 Ehlmann B. L., Mustard J. F., Murchie S. L., Bibring J.-P., Meunier A., Fraeman A. A. and
577 Langevin Y. (2011) Subsurface water and clay mineral formation during the early
578 history of Mars. *Nature* **479**, 53–60.

579 Erukhimovitch V., Pavlov V., Talyshinsky M., Souprun Y. and Huleihel M. (2005) FTIR
580 microscopy as a method for identification of bacterial and fungal infections. *Journal of*
581 *Pharmaceutical and Biomedical Analysis* **37**, 1105–1108.

582 Espitalié J., Marquis F. and Barsony I. (1984) Geochemical logging. In *Analytical Pyrolysis*
583 (ed. K. J. Voorhees). Butterworth-Heinemann. pp. 276–304.

584 Faghihzadeh F., Anaya N. M., Schifman L. A. and Oyanedel-Craver V. (2016) Fourier
585 transform infrared spectroscopy to assess molecular-level changes in microorganisms
586 exposed to nanoparticles. *Nanotechnol. Environ. Eng.* **1**, 1.

587 Farley K. A., Williford K. H., Stack K. M., Bhartia R., Chen A., de la Torre M., Hand K.,
588 Goreva Y., Herd C. D. K., Hueso R., Liu Y., Maki J. N., Martinez G., Moeller R. C.,
589 Nelessen A., Newman C. E., Nunes D., Ponce A., Spanovich N., Willis P. A., Beegle
590 L. W., Bell J. F., Brown A. J., Hamran S.-E., Hurowitz J. A., Maurice S., Paige D. A.,
591 Rodriguez-Manfredi J. A., Schulte M. and Wiens R. C. (2020) Mars 2020 mission
592 overview. *Space Sci Rev* **216**, 142.

593 Filip Z., Hermann S. and Demnerová K. (2008) FT-IR spectroscopic characteristics of
594 differently cultivated Escherichia coli. *Czech J. Food Sci.* **26**, 458–463.

595 Fornaro T., Boosman A., Brucato J. R., ten Kate I. L., Siljeström S., Poggiali G., Steele A. and
596 Hazen R. M. (2018) UV irradiation of biomarkers adsorbed on minerals under Martian-
597 like conditions: hints for life detection on Mars. *Icarus* **313**, 38–60.

598 Foustoukos D. I. and Stern J. C. (2012) Oxidation pathways for formic acid under low
599 temperature hydrothermal conditions: implications for the chemical and isotopic
600 evolution of organics on Mars. *Geochimica et Cosmochimica Acta* **76**, 14–28.

601 Fox A. C., Eigenbrode J. L. and Freeman K. H. (2019) Radiolysis of macromolecular organic
602 material in Mars-relevant mineral matrices. *Journal of Geophysical Research: Planets*
603 **124**, 3257–3266.

604 Galimov E. (2012) *The Biological Fractionation of Isotopes*., Elsevier.

605 Garip S., Bozoglu F. and Severcan F. (2007) Differentiation of mesophilic and thermophilic
606 bacteria with Fourier Transform Infrared Spectroscopy. *Applied spectroscopy* **61**, 186–
607 92.

608 Gil-Lozano C., Fairén A. G., Muñoz-Iglesias V., Fernández-Sampedro M., Prieto-Ballesteros
609 O., Gago-Duport L., Losa-Adams E., Carrizo D., Bishop J. L., Fornaro T. and Mateo-
610 Martí E. (2020) Constraining the preservation of organic compounds in Mars analog
611 nontronites after exposure to acid and alkaline fluids. *Sci Rep* **10**, 15097.

612 Goetz W., Brinckerhoff W. B., Arevalo R., Freissinet C., Getty S., Glavin D. P., Siljeström S.,
613 Buch A., Stalport F., Grubisic A., Li X., Pinnick V., Danell R., van Amerom F. H. W.,
614 Goesmann F., Steininger H., Grand N., Raulin F., Szopa C., Meierhenrich U., Brucato
615 J. R., and the MOMA Science Team (2016) MOMA: the challenge to search for
616 organics and biosignatures on Mars. *International Journal of Astrobiology* **15**, 239–250.

617 Goldstein T. P. (1983) Geocatalytic reactions in formation and maturation of petroleum.
618 *Bulletin* **67**.

619 Grotzinger J. P., Sumner D. Y., Kah L. C., Stack K., Gupta S., Edgar L., Rubin D., Lewis K.,
620 Schieber J., Mangold N., Milliken R., Conrad P. G., DesMarais D., Farmer J., Siebach
621 K., Calef F., Hurowitz J., McLennan S. M., Ming D., Vaniman D., Crisp J., Vasavada
622 A., Edgett K. S., Malin M., Blake D., Gellert R., Mahaffy P., Wiens R. C., Maurice S.,
623 Grant J. A., Wilson S., Anderson R. C., Beegle L., Arvidson R., Hallet B., Sletten R. S.,
624 Rice M., Bell J., Griffes J., Ehlmann B., Anderson R. B., Bristow T. F., Dietrich W. E.,
625 Dromart G., Eigenbrode J., Fraeman A., Hardgrove C., Herkenhoff K., Jandura L.,
626 Kocurek G., Lee S., Leshin L. A., Leveille R., Limonadi D., Maki J., McCloskey S.,
627 Meyer M., Minitti M., Newsom H., Oehler D., Okon A., Palucis M., Parker T., Rowland
628 S., Schmidt M., Squyres S., Steele A., Stolper E., Summons R., Treiman A., Williams
629 R., Yingst A., Team M. S., Kemppinen O., Bridges N., Johnson J. R., Cremers D.,
630 Godber A., Wadhwa M., Wellington D., McEwan I., Newman C., Richardson M.,
631 Charpentier A., Peret L., King P., Blank J., Weigle G., Li S., Robertson K., Sun V.,
632 Baker M., Edwards C., Farley K., Miller H., Newcombe M., Pilorget C., Brunet C.,
633 Hipkin V., Léveillé R., Marchand G., Sánchez P. S., Favot L., Cody G., Flückiger L.,
634 Lees D., Nefian A., Martin M., Gailhanou M., Westall F., Israël G., Agard C., Baroukh
635 J., Donny C., Gaboriaud A., Guillemot P., Lafaille V., Lorigny E., Paillet A., Pérez R.,
636 Saccoccio M., Yana C., Armiens-Aparicio C., Rodríguez J. C., Blázquez I. C., Gómez
637 F. G., Gómez-Elvira J., Hettrich S., Malvitte A. L., Jiménez M. M., Martínez-Frías J.,
638 Martín-Soler J., Martín-Torres F. J., Jurado A. M., Mora-Sotomayor L., Caro G. M.,
639 López S. N., Peinado-González V., Pla-García J., Manfredi J. A. R., Romeral-Planelló
640 J. J., Fuentes S. A. S., Martinez E. S., Redondo J. T., Urqui-O'Callaghan R., Mier M.-
641 P. Z., Chipera S., Lacour J.-L., Mauchien P., Sirven J.-B., Manning H., Fairén A., Hayes

A., Joseph J., Sullivan R., Thomas P., Dupont A., Lundberg A., Melikechi N., Mezzacappa A., DeMarines J., Grinspoon D., Reitz G., Prats B., Atlaskin E., Genzer M., Harri A.-M., Haukka H., Kahanpää H., Kauhanen J., Paton M., Polkko J., Schmidt W., Siili T., Fabre C., Wray J., Wilhelm M. B., Poitrasson F., Patel K., Gorevan S., Indyk S., Paulsen G., Bish D., Gondet B., Langevin Y., Geffroy C., Baratoux D., Berger G., Cros A., d'Uston C., Forni O., Gasnault O., Lasue J., Lee Q.-M., Meslin P.-Y., Pallier E., Parot Y., Pinet P., Schröder S., Toplis M., Lewin É., Brunner W., Heydari E., Achilles C., Sutter B., Cabane M., Coscia D., Szopa C., Robert F., Sautter V., Le Mouélic S., Nachon M., Buch A., Stalport F., Coll P., François P., Raulin F., Teinturier S., Cameron J., Clegg S., Cousin A., DeLapp D., Dingler R., Jackson R. S., Johnstone S., Lanza N., Little C., Nelson T., Williams R. B., Jones A., Kirkland L., Baker B., Cantor B., Caplinger M., Davis S., Duston B., Fay D., Harker D., Herrera P., Jensen E., Kennedy M. R., Krezoski G., Krysak D., Lipkaman L., McCartney E., McNair S., Nixon B., Posiolova L., Ravine M., Salamon A., Saper L., Stoiber K., Supulver K., Van Beek J., Van Beek T., Zimdar R., French K. L., Iagnemma K., Miller K., Goesmann F., Goetz W., Hviid S., Johnson M., Lefavor M., Lyness E., Breves E., Dyar M. D., Fassett C., Edwards L., Haberle R., Hoehler T., Hollingsworth J., Kahre M., Keely L., McKay C., Bleacher L., Brinckerhoff W., Choi D., Dworkin J. P., Floyd M., Freissinet C., Garvin J., Glavin D., Harpold D., Martin D. K., McAdam A., Pavlov A., Raaen E., Smith M. D., Stern J., Tan F., Trainer M., Posner A., Voytek M., Aubrey A., Behar A., Blaney D., Brinza D., Christensen L., DeFlores L., Feldman J., Feldman S., Flesch G., Jun I., Keymeulen D., Mischna M., Morookian J. M., Pavri B., Schoppers M., Sengstacken A., Simmonds J. J., Spanovich N., Juarez M. de la T., Webster C. R., Yen A., Archer P. D., Cucinotta F., Jones J. H., Morris R. V., Niles P., Rampe E., Nolan T., Fisk M., Radziemski L., Barraclough B., Bender S., Berman D., Dobrea E. N., Tokar R., Cleghorn T., Huntress W., Manhès G., Hudgins J., Olson T., Stewart N., Sarrazin P., Vicenzi E., Bullock M., Ehresmann B., Hamilton V., Hassler D., Peterson J., Rafkin S., Zeitlin C., Fedosov F., Golovin D., Karpushkina N., Kozyrev A., Litvak M., Malakhov A., Mitrofanov I., Mokrousov M., Nikiforov S., Prokhorov V., Sanin A., Tretyakov V., Varenikov A., Vostrukhin A., Kuzmin R., Clark B., Wolff M., Botta O., Drake D., Bean K., Lemmon M., Schwenzer S. P., Lee E. M., Sucharski R., Hernández M. Á. de P., Ávalos J. J. B., Ramos M., Kim M.-H., Malespin C., Plante I., Muller J.-P., Navarro-González R., Ewing R., Boynton W., Downs R., Fitzgibbon M., Harshman K., Morrison S., Kortmann O., Williams A., Lugmair G., Wilson M. A., Jakosky B., Balic-Zunic T., Frydenvang J., Jensen J. K., Kinch K., Koefoed A., Madsen M. B., Stipp S. L. S., Boyd N., Campbell J. L., Perrett G., Pradler I., VanBommel S., Jacob S., Owen T., Savijärvi H., Boehm E., Böttcher S., Burmeister S., Guo J., Köhler J., García C. M., Mueller-Mellin R., Wimmer-Schweingruber R., Bridges J. C., McConnochie T., Benna M., Franz H., Bower H., Brunner A., Blau H., Boucher T., Carmosino M., Atreya S., Elliott H., Halleaux D., Rennó N., Wong M., Pepin R., Elliott B., Spray J., Thompson L., Gordon S., Ollila A., Williams J., Vasconcelos P., Bentz J., Nealson K., Popa R., Moersch J., Tate C., Day M., Francis R., McCullough E., Cloutis E., ten Kate I. L., Scholes D., Slavney S., Stein T., Ward J., Berger J. and Moores J. E. (2014) A habitable fluvio-lacustrine environment at Yellowknife Bay, Gale Crater, Mars. *Science* **343**, 1242777.

Hassler D. M., Zeitlin C., Wimmer-Schweingruber R. F., Ehresmann B., Rafkin S., Eigenbrode J. L., Brinza D. E., Weigle G., Böttcher S., Böhm E., Burmeister S., Guo J., Köhler J., Martin C., Reitz G., Cucinotta F. A., Kim M.-H., Grinspoon D., Bullock M. A., Posner A., Gómez-Elvira J., Vasavada A., Grotzinger J. P., Team M. S., Kemppinen O.,

Cremers D., Bell J. F., Edgar L., Farmer J., Godber A., Wadhwa M., Wellington D., McEwan I., Newman C., Richardson M., Charpentier A., Peret L., King P., Blank J., Schmidt M., Li S., Milliken R., Robertson K., Sun V., Baker M., Edwards C., Ehlmann B., Farley K., Griffes J., Miller H., Newcombe M., Pilorget C., Rice M., Siebach K., Stack K., Stolper E., Brunet C., Hipkin V., Léveillé R., Marchand G., Sánchez P. S., Favot L., Cody G., Steele A., Flückiger L., Lees D., Nefian A., Martin M., Gailhanou M., Westall F., Israël G., Agard C., Baroukh J., Donny C., Gaboriaud A., Guillemot P., Lafaille V., Lorigny E., Paillet A., Pérez R., Saccoccio M., Yana C., Armiens-Aparicio C., Rodríguez J. C., Blázquez I. C., Gómez F. G., Hettrich S., Malvitte A. L., Jiménez M. M., Martínez-Frías J., Martín-Soler J., Martín-Torres F. J., Jurado A. M., Mora-Sotomayor L., Caro G. M., López S. N., Peinado-González V., Pla-García J., Manfredi J. A. R., Romeral-Planelló J. J., Fuentes S. A. S., Martinez E. S., Redondo J. T., Urqui-O'Callaghan R., Mier M.-P. Z., Chipera S., Lacour J.-L., Mauchien P., Sirven J.-B., Manning H., Fairén A., Hayes A., Joseph J., Squyres S., Sullivan R., Thomas P., Dupont A., Lundberg A., Melikechi N., Mezzacappa A., Berger T., Matthia D., Prats B., Atlaskin E., Genzer M., Harri A.-M., Haukka H., Kahanpää H., Kauhanen J., Kemppinen O., Paton M., Polkko J., Schmidt W., Siili T., Fabre C., Wray J., Wilhelm M. B., Poitrasson F., Patel K., Gorevan S., Indyk S., Paulsen G., Gupta S., Bish D., Schieber J., Gondet B., Langevin Y., Geffroy C., Baratoux D., Berger G., Cros A., d'Uston C., Forni O., Gasnault O., Lasue J., Lee Q.-M., Maurice S., Meslin P.-Y., Pallier E., Parot Y., Pinet P., Schröder S., Toplis M., Lewin É., Brunner W., Heydari E., Achilles C., Oehler D., Sutter B., Cabane M., Coscia D., Israël G., Szopa C., Dromart G., Robert F., Sautter V., Le Mouélic S., Mangold N., Nachon M., Buch A., Stalport F., Coll P., François P., Raulin F., Teinturier S., Cameron J., Clegg S., Cousin A., DeLapp D., Dingler R., Jackson R. S., Johnstone S., Lanza N., Little C., Nelson T., Wiens R. C., Williams R. B., Jones A., Kirkland L., Treiman A., Baker B., Cantor B., Caplinger M., Davis S., Duston B., Edgett K., Fay D., Hardgrove C., Harker D., Herrera P., Jensen E., Kennedy M. R., Krezoski G., Krysak D., Lipkaman L., Malin M., McCartney E., McNair S., Nixon B., Posiolova L., Ravine M., Salamon A., Saper L., Stoiber K., Supulver K., Van Beek J., Van Beek T., Zimdar R., French K. L., Iagnemma K., Miller K., Summons R., Goesmann F., Goetz W., Hviid S., Johnson M., Lefavor M., Lyness E., Breves E., Dyar M. D., Fassett C., Blake D. F., Bristow T., DesMarais D., Edwards L., Haberle R., Hoehler T., Hollingsworth J., Kahre M., Keely L., McKay C., Wilhelm M. B., Bleacher L., Brinckerhoff W., Choi D., Conrad P., Dworkin J. P., Floyd M., Freissinet C., Garvin J., Glavin D., Harpold D., Jones A., Mahaffy P., Martin D. K., McAdam A., Pavlov A., Raaen E., Smith M. D., Stern J., Tan F., Trainer M., Meyer M., Voytek M., Anderson R. C., Aubrey A., Beegle L. W., Behar A., Blaney D., Calef F., Christensen L., Crisp J. A., DeFlores L., Ehlmann B., Feldman J., Feldman S., Flesch G., Hurowitz J., Jun I., Keymeulen D., Maki J., Mischna M., Morookian J. M., Parker T., Pavri B., Schoppers M., Sengstacken A., Simmonds J. J., Spanovich N., Juarez M. de la T., Webster C. R., Yen A., Archer P. D., Jones J. H., Ming D., Morris R. V., Niles P., Rampe E., Nolan T., Fisk M., Radziemski L., Barraclough B., Bender S., Berman D., Dobrea E. N., Tokar R., Vaniman D., Williams R. M. E., Yingst A., Lewis K., Leshin L., Cleghorn T., Huntress W., Manhès G., Hudgins J., Olson T., Stewart N., Sarrazin P., Grant J., Vicenzi E., Wilson S. A., Hamilton V., Peterson J., Fedosov F., Golovin D., Karpushkina N., Kozyrev A., Litvak M., Malakhov A., Mitrofanov I., Mokrousov M., Nikiforov S., Prokhorov V., Sanin A., Tretyakov V., Varenikov A., Vostrukhin A., Kuzmin R., Clark B., Wolff M., McLennan S., Botta O., Drake D., Bean K., Lemmon M., Schwenzer S. P., Anderson R. B., Herkenhoff K., Lee E. M., Sucharski R., Hernández M. Á. de P., Ávalos J. J. B., Ramos M., Malespin C., Plante I., Muller J.-

P., Navarro-González R., Ewing R., Boynton W., Downs R., Fitzgibbon M., Harshman K., Morrison S., Dietrich W., Kortmann O., Palucis M., Sumner D. Y., Williams A., Lugmair G., Wilson M. A., Rubin D., Jakosky B., Balic-Zunic T., Frydenvang J., Jensen J. K., Kinch K., Koefoed A., Madsen M. B., Stipp S. L. S., Boyd N., Campbell J. L., Gellert R., Perrett G., Pradler I., VanBommel S., Jacob S., Owen T., Rowland S., Atlaskin E., Savijärvi H., García C. M., Mueller-Mellin R., Bridges J. C., McConnochie T., Benna M., Franz H., Bower H., Brunner A., Blau H., Boucher T., Carmosino M., Atreya S., Elliott H., Halleaux D., Rennó N., Wong M., Pepin R., Elliott B., Spray J., Thompson L., Gordon S., Newsom H., Ollila A., Williams J., Vasconcelos P., Bentz J., Nealson K., Popa R., Kah L. C., Moersch J., Tate C., Day M., Kocurek G., Hallet B., Sletten R., Francis R., McCullough E., Cloutis E., ten Kate I. L., Kuzmin R., Arvidson R., Fraeman A., Scholes D., Slavney S., Stein T., Ward J., Berger J. and Moores J. E. (2014) Mars' surface radiation environment measured with the Mars Science Laboratory's Curiosity rover. *Science* **343**, 1244797.

Hayes J. M. (1993) Factors controlling 13C contents of sedimentary organic compounds: principles and evidence. *Marine Geology* **113**, 111–125.

Hayes J. M. (2001) Fractionation of carbon and hydrogen Isotopes in biosynthetic processes. *Reviews in Mineralogy and Geochemistry* **43**, 225–277.

Hays L. E., Graham H. V., Des Marais D. J., Hausrath E. M., Horgan B., McCollom T. M., Parenteau M. N., Potter-McIntyre S. L., Williams A. J. and Lynch K. L. (2017) Biosignature preservation and detection in Mars analog environments. *Astrobiology* **17**, 363–400.

Hecht M. H., Kounaves S. P., Quinn R. C., West S. J., Young S. M. M., Ming D. W., Catling D. C., Clark B. C., Boynton W. V., Hoffman J., DeFlores L. P., Gospodinova K., Kapit J. and Smith P. H. (2009) Detection of perchlorate and the soluble chemistry of Martian soil at the Phoenix lander site. *Science* **325**, 64–67.

Hedges J. I. and Keil R. G. (1995) Sedimentary organic matter preservation: an assessment and speculative synthesis. *Marine Chemistry* **49**, 81–115.

Hong J., Yang H., Pang D., Wei L. and Deng C. (2018) Effects of mono- and di-valent metal cations on the morphology of lipid vesicles. *Chemistry and Physics of Lipids* **217**, 19–28.

Horita J. (2005) Some perspectives on isotope biosignatures for early life. *Chemical Geology* **218**, 171–186.

Horsfield B. and Douglas A. G. (1980) The influence of minerals on the pyrolysis of kerogens. *Geochimica et Cosmochimica Acta* **44**, 1119–1131.

Hurowitz J. A., Grotzinger J. P., Fischer W. W., McLennan S. M., Milliken R. E., Stein N., Vasavada A. R., Blake D. F., Dehouck E., Eigenbrode J. L., Fairén A. G., Frydenvang J., Gellert R., Grant J. A., Gupta S., Herkenhoff K. E., Ming D. W., Rampe E. B., Schmidt M. E., Siebach K. L., Stack-Morgan K., Sumner D. Y. and Wiens R. C. (2017) Redox stratification of an ancient lake in Gale crater, Mars. *Science* **356**, eaah6849.

Igisu M., Yokoyama T., Ueno Y., Nakashima S., Shimojima M., Ohta H. and Maruyama S. (2018) Changes of aliphatic C–H bonds in cyanobacteria during experimental thermal

783 maturation in the presence or absence of silica as evaluated by FTIR microspectroscopy.
784 *Geobiology* **16**, 412–428.

785 Ivanov B. A. and Pierazzo E. (2011) Impact cratering in H2O-bearing targets on Mars: Thermal
786 field under craters as starting conditions for hydrothermal activity: thermal field under
787 Martian impact craters. *Meteoritics & Planetary Science* **46**, 601–619.

788 Jacquemot P., Viennet J.-C., Bernard S., Le Guillou C., Rigaud B., Delbes L., Georgelin T. and
789 Jaber M. (2019) The degradation of organic compounds impacts the crystallization of
790 clay minerals and vice versa. *Sci Rep* **9**, 20251.

791 Johns W. D. (1979) Clay mineral catalysis and petroleum generation. *Annu. Rev. Earth Planet.*
792 *Sci.* **7**, 183–198.

793 Johnston C. T., de Oliveira M. F., Teppen B. J., Sheng G. and Boyd S. A. (2001) Spectroscopic
794 study of nitroaromatic−smectite sorption mechanisms. *Environ. Sci. Technol.* **35**, 4767–
795 4772.

796 Joshi P. C., Dubey K., Aldersley M. F. and Sausville M. (2015) Clay catalyzed RNA synthesis
797 under Martian conditions: application for Mars return samples. *Biochemical and*
798 *Biophysical Research Communications* **462**, 99–104.

799 Kennedy M. J., Pevear D. R. and Hill R. J. (2002) Mineral surface control of organic carbon in
800 black shale. *Science* **295**, 657–660.

801 Kleber M., Bourg I. C., Coward E. K., Hansel C. M., Myneni S. C. B. and Nunan N. (2021)
802 Dynamic interactions at the mineral–organic matter interface. *Nat Rev Earth Environ* **2**,
803 402–421.

804 Kloprogge and Frost R. L. (2000) The effect of synthesis temperature on the FT-Raman and
805 FT-IR spectra of saponites - UQ eSpace.

806 Kloprogge J. T. and Ponce C. P. (2021) Spectroscopic studies of synthetic and natural saponites:
807 a review. *Minerals* **11**, 112.

808 Kopittke P. M., Hernandez-Soriano M. C., Dalal R. C., Finn D., Menzies N. W., Hoeschen C.
809 and Mueller C. W. (2018) Nitrogen-rich microbial products provide new organo-
810 mineral associations for the stabilization of soil organic matter. *Global Change Biology*
811 **24**, 1762–1770.

812 Kral T. A., Birch W., Lavender L. E. and Virden B. T. (2014) Potential use of highly insoluble
813 carbonates as carbon sources by methanogens in the subsurface of Mars. *Planetary and*
814 *Space Science* **101**, 181–185.

815 Kronyak R. E., Kah L. C., Edgett K. S., VanBommel S. J., Thompson L. M., Wiens R. C., Sun
816 V. Z. and Nachon M. (2019) Mineral-filled fractures as indicators of multigenerational
817 fluid flow in the Pahrump Hills member of the Murray Formation, Gale Crater, Mars.
818 *Earth and Space Science* **6**, 238–265.

819 Lagaly G. (1984) Clay-organic interactions. *Philosophical Transactions of the Royal Society of*
820 *London. Series A, Mathematical and Physical Sciences* **311**, 315–332.

Lagaly G., Ogawa M. and Dékány I. (2006) Clay mineral organic interactions. In *Developments in Clay Science* Elsevier. pp. 309–377.

Laird D. A., Scott A. D. and Fenton T. E. (1989) Evaluation of the alkylammonium method of determining layer charge. *Clays and Clay Minerals*.

Lanson B., Mignon P., Velde M., Bauer A., Lanson M., Findling N. and Perez del Valle C. (2022) Determination of layer charge density in expandable phyllosilicates with alkylammonium ions: a combined experimental and theoretical assessment of the method. *Applied Clay Science* **229**, 106665.

Lasne J., Noblet A., Szopa C., Navarro-González R., Cabane M., Poch O., Stalport F., François P., Atreya S. k. and Coll P. (2016) Oxidants at the surface of Mars: a review in light of recent exploration results. *Astrobiology* **16**, 977–996.

Legal J. M., Manfait M. and Theophanides T. (1991) Applications of FTIR spectroscopy in structural studies of cells and bacteria. *Journal of Molecular Structure* **242**, 397–407.

Leshin L. A., Mahaffy P. R., Webster C. R., Cabane M., Coll P., Conrad P. G., Archer P. D., Atreya S. K., Brunner A. E., Buch A., Eigenbrode J. L., Flesch G. J., Franz H. B., Freissinet C., Glavin D. P., McAdam A. C., Miller K. E., Ming D. W., Morris R. V., Navarro-González R., Niles P. B., Owen T., Pepin R. O., Squyres S., Steele A., Stern J. C., Summons R. E., Sumner D. Y., Sutter B., Szopa C., Teinturier S., Trainer M. G., Wray J. J., Grotzinger J. P., and MSL Science Team (2013) Volatile, isotope, and organic analysis of martian fines with the Mars Curiosity rover. *Science* **341**, 1238937.

Levin G. V. and Straat P. A. (1977) Life on Mars? The Viking labeled release experiment. *Biosystems* **9**, 165–174.

Lewan M. D. and Roy S. (2011) Role of water in hydrocarbon generation from Type-I kerogen in Mahogany oil shale of the Green River Formation. *Organic Geochemistry* **42**, 31–41.

Li J., Bernard S., Benzerara K., Beyssac O., Allard T., Cosmidis J. and Moussou J. (2014) Impact of biomineralization on the preservation of microorganisms during fossilization: an experimental perspective. *Earth and Planetary Science Letters* **400**, 113–122.

Lugtenberg B. (1981) Composition and function of the outer membrane of Escherichia coli. *Trends in Biochemical Sciences* **6**, 262–266.

Macko S. A., Fogel M. L., Hare P. E. and Hoering T. C. (1987) Isotopic fractionation of nitrogen and carbon in the synthesis of amino acids by microorganisms. *Chemical Geology: Isotope Geoscience section* **65**, 79–92.

Madejová J., Gates W. P. and Petit S. (2017) IR spectra of clay minerals. In *Developments in Clay Science* Elsevier. pp. 107–149.

McCollom T. M. and Seewald J. S. (2006) Carbon isotope composition of organic compounds produced by abiotic synthesis under hydrothermal conditions. *Earth and Planetary Science Letters* **243**, 74–84.

McCollom T. M., Seewald J. S. and Simoneit B. R. T. (2001) Reactivity of monocyclic aromatic compounds under hydrothermal conditions. *Geochimica et Cosmochimica Acta* **65**, 455–468.

McKay D. S., Gibson E. K., Thomas-Keprta K. L., Vali H., Romanek C. S., Clemett S. J., Chillier X. D., Maechling C. R. and Zare R. N. (1996) Search for past life on Mars: possible relic biogenic activity in martian meteorite ALH84001. *Science* **273**, 924–930.

McMahon S. (2018) The chemistry of fossilization on Earth and Mars. *The Biochemist* **40**, 28–32.

McMahon S., Bosak T., Grotzinger J. P., Milliken R. E., Summons R. E., Daye M., Newman S. A., Fraeman A., Williford K. H. and Briggs D. E. G. (2018) A field guide to finding fossils on Mars. *JGR Planets* **123**, 1012–1040.

McSween H. Y. (2019) The Search for Biosignatures in Martian Meteorite Allan Hills 84001. In *Biosignatures for Astrobiology* (eds. B. Cavalazzi and F. Westall). Advances in astrobiology and biogeophysics. Springer International Publishing, Cham. pp. 167–182.

Megevand V., Viennet J. c., Balan E., Gauthier M., Rosier P., Morand M., Garino Y., Guillaumet M., Pont S., Beyssac O. and Bernard S. (2021) Impact of UV radiation on the raman signal of cystine: implications for the detection of S-rich organics on Mars. *Astrobiology* **21**, 566–574.

Miot J., Bernard S., Bourreau M., Guyot F. and Kish A. (2017) Experimental maturation of Archaea encrusted by Fe-phosphates. *Sci Rep* **7**, 16984.

Monnard P.-A., Apel C. L., Kanavarioti A. and Deamer D. W. (2002) Influence of ionic inorganic solutes on self-assembly and polymerization processes related to early forms of life: implications for a prebiotic aqueous medium. *Astrobiology* **2**, 139–152.

Nadtochenko V. A., Rincon A. G., Stanca S. E. and Kiwi J. (2005) Dynamics of E. coli membrane cell peroxidation during TiO2 photocatalysis studied by ATR-FTIR spectroscopy and AFM microscopy. *Journal of Photochemistry and Photobiology A: Chemistry* **169**, 131–137.

Nikaido H. (2003) Molecular basis of bacterial outer membrane permeability revisited. *Microbiol Mol Biol Rev* **67**, 593–656.

Nikalje M. D., Phukan P. and Sudalai A. (2000) Rencent advances in clay-catalyzed organic transformations. *Organic Preparations and Procedures International* **32**, 1–40.

Nyarko E. B., Puzey K. A. and Donnelly C. W. (2014) Rapid differentiation of listeria monocytogenes epidemic clones III and IV and their intact compared with heat-killed populations using Fourier Transform Infrared Spectroscopy and chemometrics. *Journal of Food Science* **79**, M1189–M1196.

Oehler J. H. and Schopf J. W. (1971) Artificial microfossils: experimental studies of permineralization of blue-green algae in silica. *Science* **174**, 1229–1231.

Osinski G. R., Tornabene L. L., Banerjee N. R., Cockell C. S., Flemming R., Izawa M. R. M., McCutcheon J., Parnell J., Preston L. J., Pickersgill A. E., Pontefract A., Sapers H. M.

and Southam G. (2013) Impact-generated hydrothermal systems on Earth and Mars. *Icarus* **224**, 347–363.

Pajola M., Rossato S., Baratti E., Pozzobon R., Quantin C., Carter J. and Thollot P. (2017) Boulder abundances and size-frequency distributions on Oxia Planum-Mars: scientific implications for the 2020 ESA ExoMars rover. *Icarus* **296**, 73–90.

Pérez-Maqueda L. A., Sánchez-Jiménez P. E., Perejón A., García-Garrido C., Criado J. M. and Benítez-Guerrero M. (2014) Scission kinetic model for the prediction of polymer pyrolysis curves from chain structure. *Polymer Testing* **37**, 1–5.

Picard A., Kappler A., Schmid G., Quaroni L. and Obst M. (2015) Experimental diagenesis of organo-mineral structures formed by microaerophilic Fe(II)-oxidizing bacteria. *Nat Commun* **6**, 6277.

Piqueux S., Buz J., Edwards C. S., Bandfield J. L., Kleinböhl A., Kass D. M. and Hayne P. O. (2019) Widespread shallow water ice on Mars at high latitudes and mid-latitudes. *Geophysical Research Letters* **46**, 14,290-14,298.

Pusch R. and Karnland O. (1988) *Hydrothermal effects on montmorillonite*., Sweden.

Quantin-Nataf C., Carter J., Mandon L., Thollot P., Balme M., Volat M., Pan L., Loizeau D., Millot C., Breton S., Dehouck E., Fawdon P., Gupta S., Davis J., Grindrod P. M., Pacifici A., Bultel B., Allemand P., Ody A., Lozach L. and Broyer J. (2021) Oxia Planum: the landing site for the ExoMars "Rosalind Franklin" rover mission: Geological context and prelanding interpretation. *Astrobiology* **21**, 345–366.

Quinn R. C., Martucci H. F. H., Miller S. R., Bryson C. E., Grunthaner F. J. and Grunthaner P. J. (2013) Perchlorate radiolysis on Mars and the origin of Martian soil reactivity. *Astrobiology* **13**, 515–520.

Rahman H. M., Kennedy M., Löhr S., Dewhurst D. N., Sherwood N., Yang S. and Horsfield B. (2018) The influence of shale depositional fabric on the kinetics of hydrocarbon generation through control of mineral surface contact area on clay catalysis. *Geochimica et Cosmochimica Acta* **220**, 429–448.

Rathbun J. A. and Squyres S. W. (2002) Hydrothermal systems associated with Martian impact craters. *Icarus* **157**, 362–372.

Rothenberg G., Downie A. P., Raston C. L. and Scott J. L. (2001) Understanding solid/solid organic reactions. *J. Am. Chem. Soc.* **123**, 8701–8708.

Ruiz N. and Silhavy T. J. (2022) How Escherichia coli became the flagship bacterium of molecular biology. *Journal of Bacteriology* **204**, e00230-22.

Salvatore M. R., Goudge T. A., Bramble M. S., Edwards C. S., Bandfield J. L., Amador E. S., Mustard J. F. and Christensen P. R. (2018) Bulk mineralogy of the NE Syrtis and Jezero crater regions of Mars derived through thermal infrared spectral analyses. *Icarus* **301**, 76–96.

Samie A. (2017) *Escherichia coli: Recent Advances on Physiology, Pathogenesis and Biotechnological Applications*., BoD – Books on Demand.

936 Sánchez-Jiménez P. E., Pérez-Maqueda L. A., Perejón A. and Criado J. M. (2010) Generalized
937 kinetic master plots for the thermal degradation of polymers following a random
938 scission mechanism. *J Phys Chem A* **114**, 7868–7876.

939 van Santen R. A. and Liu C. (2018) Theory of zeolite catalysis. In *Modelling and Simulation in*
940 *the Science of Micro- and Meso-Porous Materials* Elsevier. pp. 151–188.

941 Schiffbauer J. D., Wallace A. F., Hunter Jr J. L., Kowalewski M., Bodnar R. J. and Xiao S.
942 (2012) Thermally-induced structural and chemical alteration of organic-walled
943 microfossils: an experimental approach to understanding fossil preservation in
944 metasediments. *Geobiology* **10**, 402–423.

945 Schwenzer S. P., Bridges J. C., Wiens R. C., Conrad P. G., Kelley S. P., Leveille R., Mangold
946 N., Martín-Torres J., McAdam A., Newsom H., Zorzano M. P., Rapin W., Spray J.,
947 Treiman A. H., Westall F., Fairén A. G. and Meslin P.-Y. (2016) Fluids during
948 diagenesis and sulfate vein formation in sediments at Gale crater, Mars. *Meteorit Planet*
949 *Sci* **51**, 2175–2202.

950 Segura T. L., Toon O. B., Colaprete A. and Zahnle K. (2002) Environmental effects of large
951 impacts on Mars. *Science* **298**, 1977–1980.

952 Sinton W. M. (1957) Spectroscopic evidence for vegetation on Mars. *The Astrophysical Journal*
953 **126**, 231.

954 Sinton W. M. (1959) Further evidence of vegetation on Mars: the presence of large organic
955 molecules is indicated by recent infrared-spectroscopic tests. *Science* **130**, 1234–1237.

956 Sohlenkamp C. and Geiger O. (2016) Bacterial membrane lipids: diversity in structures and
957 pathways ed. F. Narberhaus. *FEMS Microbiology Reviews* **40**, 133–159.

958 Spiker E. C. and Hatcher P. G. (1984) Carbon isotope fractionation of sapropelic organic matter
959 during early diagenesis. *Organic Geochemistry* **5**, 283–290.

960 Stalport F., Coll P., Szopa C., Cottin H. and Raulin F. (2009) Investigating the photostability
961 of carboxylic acids exposed to Mars surface ultraviolet radiation conditions.
962 *Astrobiology* **9**, 543–549.

963 Stalport F., Rouquette L., Poch O., Dequaire T., Chaouche-Mechidal N., Payart S., Szopa C.,
964 Coll P., Chaput D., Jaber M., Raulin F. and Cottin H. (2019) The Photochemistry on
965 Space Station (PSS) experiment: organic matter under Mars-like surface UV radiation
966 conditions in low Earth orbit. *Astrobiology* **19**, 1037–1052.

967 Summons R. E., Albrecht P., McDonald G. and Moldowan J. M. (2008) Molecular
968 biosignatures. *Space Sci Rev* **135**, 133–159.

969 Summons R. E., Amend J. P., Bish D., Buick R., Cody G. D., Des Marais D. J., Dromart G.,
970 Eigenbrode J. L., Knoll A. H. and Sumner D. Y. (2011) Preservation of martian organic
971 and environmental records: final report of the Mars biosignature working group.
972 *Astrobiology* **11**, 157–181.

973 Taj M. K., Samreen Z., Ling J. X., Taj I., Hassani T. M. and Yunlin W. (2014) Escherichia coli
974 as a model organism.

Tan J. S. W., Royle S. H. and Sephton M. A. (2021) Artificial maturation of iron- and sulfur-rich Mars analogues: implications for the diagenetic stability of biopolymers and their detection with Pyrolysis–Gas Chromatography–Mass Spectrometry. *Astrobiology* **21**, 199–218.

Vago J. L., Westall F., Pasteur Instrument Teams, Landing S, Coates A. J., Jaumann R., Korablev O., Ciarletti V., Mitrofanov I., Josset J.-L., De Sanctis M. C., Bibring J.-P., Rull F., Goesmann F., Steininger H., Goetz W., Brinckerhoff W., Szopa C., Raulin F., Westall F., Edwards H. G. M., Whyte L. G., Fairén A. G., Bibring J.-P., Bridges J., Hauber E., Ori G. G., Werner S., Loizeau D., Kuzmin R. O., Williams R. M. E., Flahaut J., Forget F., Vago J. L., Rodionov D., Korablev O., Svedhem H., Sefton-Nash E., Kminek G., Lorenzoni L., Joudrier L., Mikhailov V., Zashchirinskiy A., Alexashkin S., Calantropio F., Merlo A., Poulakis P., Witasse O., Bayle O., Bayón S., Meierhenrich U., Carter J., García-Ruiz J. M., Baglioni P., Haldemann A., Ball A. J., Debus A., Lindner R., Haessig F., Monteiro D., Trautner R., Voland C., Rebeyre P., Goulty D., Didot F., Durrant S., Zekri E., Koschny D., Toni A., Visentin G., Zwick M., van Winnendael M., Azkarate M., Carreau C., and the ExoMars Project Team (2017) Habitability on early Mars and the search for biosignatures with the ExoMars rover. *Astrobiology* **17**, 471–510.

Vandenbroucke M. and Largeau C. (2007) Kerogen origin, evolution and structure. *Organic Geochemistry* **38**, 719–833.

Viennet J.-C., Bernard S., Le Guillou C., Jacquemot P., Balan E., Delbes L., Rigaud B., Georgelin T. and Jaber M. (2019) Experimental clues for detecting biosignatures on Mars. *Geochem. Persp. Let.*, 28–33.

Viennet J.-C., Bernard S., Le Guillou C., Jacquemot P., Delbes L., Balan E. and Jaber M. (2020) Influence of the nature of the gas phase on the degradation of RNA during fossilization processes. *Applied Clay Science* **191**, 105616.

Viennet J.-C., Le Guillou C., Remusat L., Baron F., Delbes L., Blanchenet A. M., Laurent B., Criouet I. and Bernard S. (2022) Experimental investigation of Fe-clay/organic interactions under asteroidal conditions. *Geochimica et Cosmochimica Acta* **318**, 352–365.

Vinogradoff V., Le Guillou C., Bernard S., Viennet J. C., Jaber M. and Remusat L. (2020a) Influence of phyllosilicates on the hydrothermal alteration of organic matter in asteroids: Experimental perspectives. *Geochimica et Cosmochimica Acta* **269**, 150–166.

Vinogradoff V., Remusat L., McLain H. L., Aponte J. C., Bernard S., Danger G., Dworkin J. P., Elsila J. E. and Jaber M. (2020b) Impact of phyllosilicates on amino acid formation under asteroidal conditions. *ACS Earth Space Chem.* **4**, 1398–1407.

Wang J., Ma W. and Wang X. (2021) Insights into the structure of Escherichia coli outer membrane as the target for engineering microbial cell factories. *Microb Cell Fact* **20**, 73.

Westall F. and Cockell C. S. (2016) Biosignatures for astrobiology. *Orig Life Evol Biosph* **46**, 105–106.

Westall F., Loizeau D., Foucher F., Bost N., Betrand M., Vago J. and Kminek G. (2013) Habitability on Mars from a microbial point of view. *Astrobiology* **13**, 887–897.

Westall F., Foucher F., Bost N., Bertrand M., Loizeau D., Vago J. L., Kminek G., Gaboyer F., Campbell K. A., Bréhéret J.-G., Gautret P. and Cockell C. S. (2015) Biosignatures on Mars: What, Where, and How? Implications for the search for Martian Life. *Astrobiology* **15**, 998–1029.

Whitney G. (1983) Hydrothermal reactivity of saponite. *Clays Clay Miner*. **31**, 1–8.

Yuan P., Liu H., Liu D., Tan D., Yan W. and He H. (2013) Role of the interlayer space of montmorillonite in hydrocarbon generation: An experimental study based on high temperature–pressure pyrolysis. *Applied Clay Science* **75–76**, 82–91.

Zhang C. L. (2002) Stable carbon isotopes of lipid biomarkers: analysis of metabolites and metabolic fates of environmental microorganisms. *Current Opinion in Biotechnology* **13**, 25–30.

Zolotov M. Yu. and Mironenko M. V. (2016) Chemical models for martian weathering profiles: Insights into formation of layered phyllosilicate and sulfate deposits. *Icarus* **275**, 203–220.

TABLE

Table 1. EA-irMS results. Note that the values of the starting materials and of the residues of experiments conducted at 150°C for 10 days are shown twice to facilitate the comparison. Standard deviations are derived from results obtained on alanine standards.

	%C ± SD	%N ± SD	N/C ± SD	$\delta^{13}C$ (‰) ± SD
E. coli (Starting Material)	46.66 ± 0.23	13.60 ± 0.05	0.25 ± 0.001	-24.74 ± 0.11
E. coli + H_2O + CO_2 - 100°C 10d	54.88 ± 0.27	13.19 ± 0.05	0.21 ± 0.001	-25.48 ± 0.11
E. coli + H_2O + CO_2 - 150°C 10d	70.27 ± 0.35	6.51 ± 0.03	0.08 ± 0.001	-27.90 ± 0.12
E. coli + H_2O + CO_2 - 200°C 10d	66.49 ± 0.33	5.30 ± 0.02	0.07 ± 0.0002	-27.77 ± 0.12
E. coli (Starting Material)	46.66 ± 0.23	13.60 ± 0.05	0.25 ± 0.001	-24.74 ± 0.11
E. coli + H_2O + CO_2 - 150°C 1d	63.10 ± 0.31	10.18 ± 0.04	0.14 ± 0.0005	-26.93 ± 0.12
E. coli + H_2O + CO_2 - 150°C 10d	70.27 ± 0.35	6.51 ± 0.03	0.08 ± 0.001	-27.90 ± 0.12
E. coli + H_2O + CO_2 - 150°C 100d	68.27 ± 0.53	5.95 ± 0.02	0.07 ± 0.0004	-27.83 ± 0.13
E. coli + Saponite (Starting Material)	12.20 ± 0.06	3.50 ± 0.03	0.25 ± 0.001	-24.96 ± 0.13
E. coli + Saponite + H_2O + CO_2 - 100°C 10d	9.54 ± 0.05	2.82 ± 0.01	0.25 ± 0.001	-24.95 ± 0.11
E. coli + Saponite + H_2O + CO_2 - 150°C 10d	5.87 ± 0.03	1.99 ± 0.01	0.29 ± 0.001	-24.65 ± 0.11
E. coli + Saponite + H_2O + CO_2 - 200°C 10d	9.13 ± 0.10	1.30 ± 0.10	0.12 ± 0.01	-26.55 ± 0.08
E. coli + Saponite (Starting Material)	12.20 ± 0.06	3.50 ± 0.03	0.25 ± 0.001	-24.96 ± 0.13
E. coli + Saponite + H_2O + CO_2 - 150°C 1d	9.15 ± 0.05	2.83 ± 0.01	0.27 ± 0.001	-25.47 ± 0.11
E. coli + Saponite + H_2O + CO_2 - 150°C 10d	5.87 ± 0.03	1.99 ± 0.01	0.29 ± 0.001	-24.65 ± 0.11
E. coli + Saponite + H_2O + CO_2 - 150°C 100d	5.65 ± 0.04	1.32 ± 0.005	0.20 ± 0.001	-25.47 ± 0.12

FIGURE CAPTIONS

Figure 1

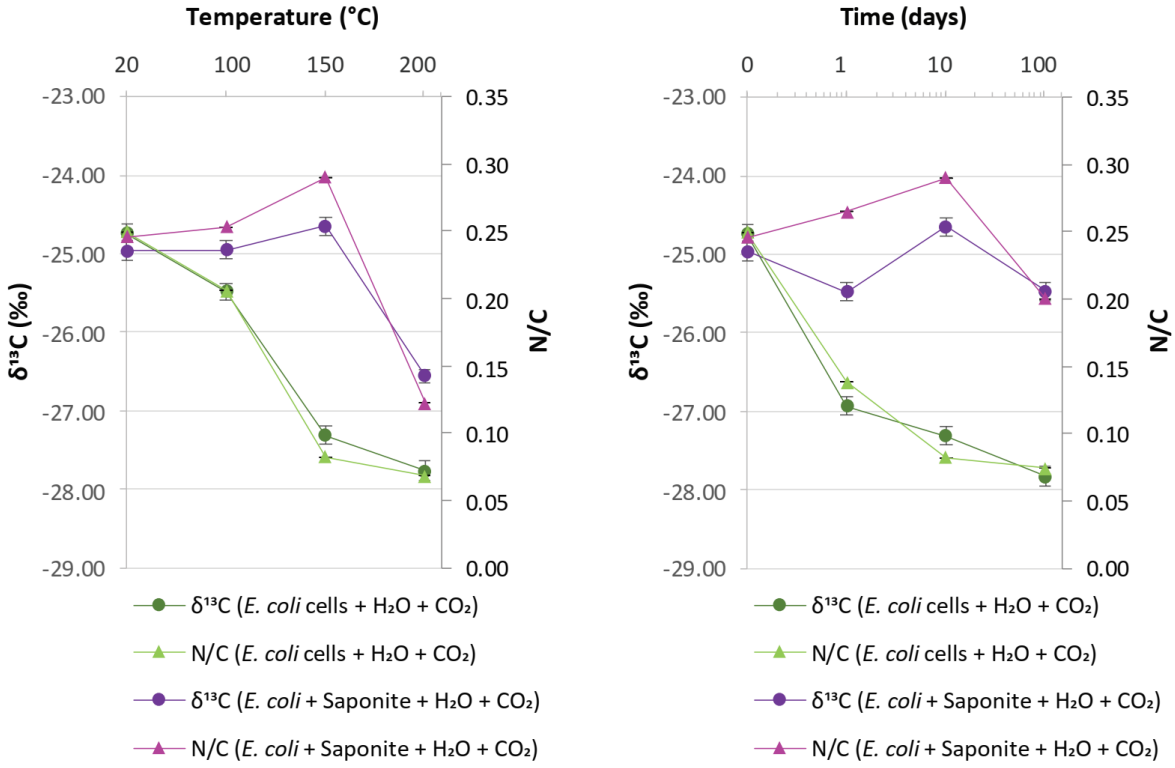

Figure 2. Evolution of the N/C and $\delta^{13}C$ values with experimental duration (left) and with experimental temperatures (right).

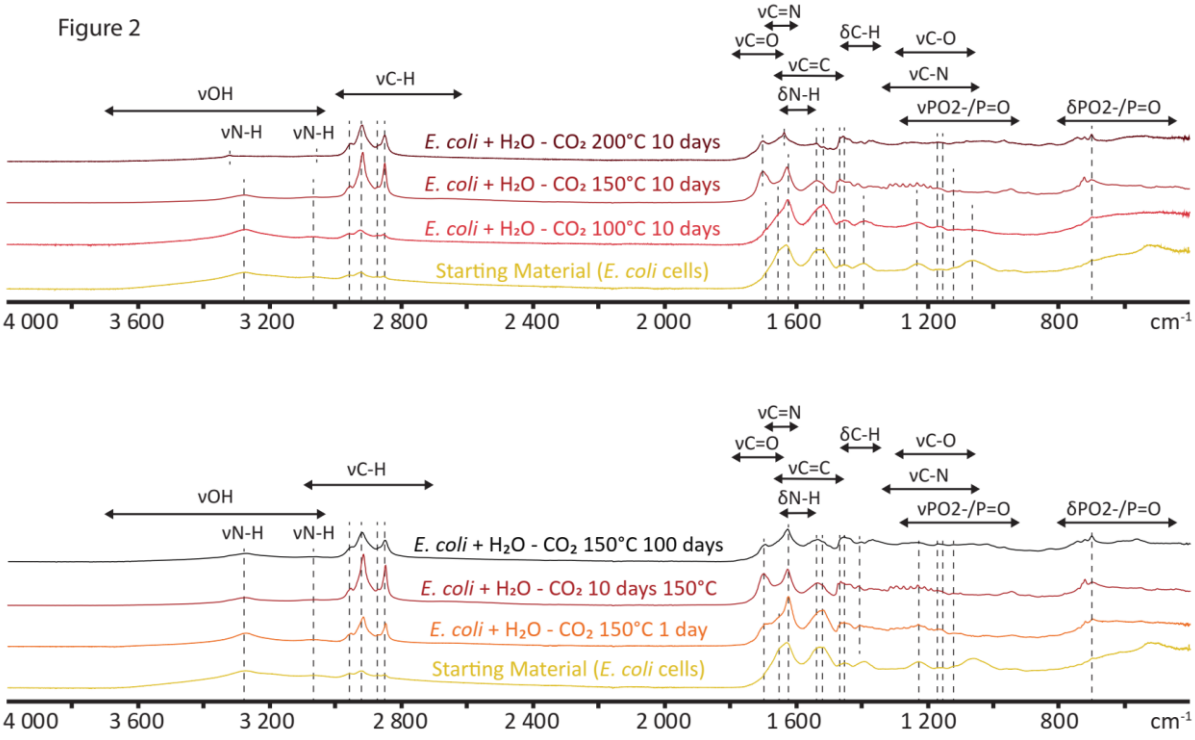

Figure 2. Mid-IR spectra of residues of experiments conducted in the absence of saponite. Note that the spectra of the starting materials (pristine *E. coli* cells) and of the residue of the experiment conducted at 150°C for 10 days are shown twice to facilitate the comparison. All spectra are normalized to the CH band at 1465 cm^{-1}.

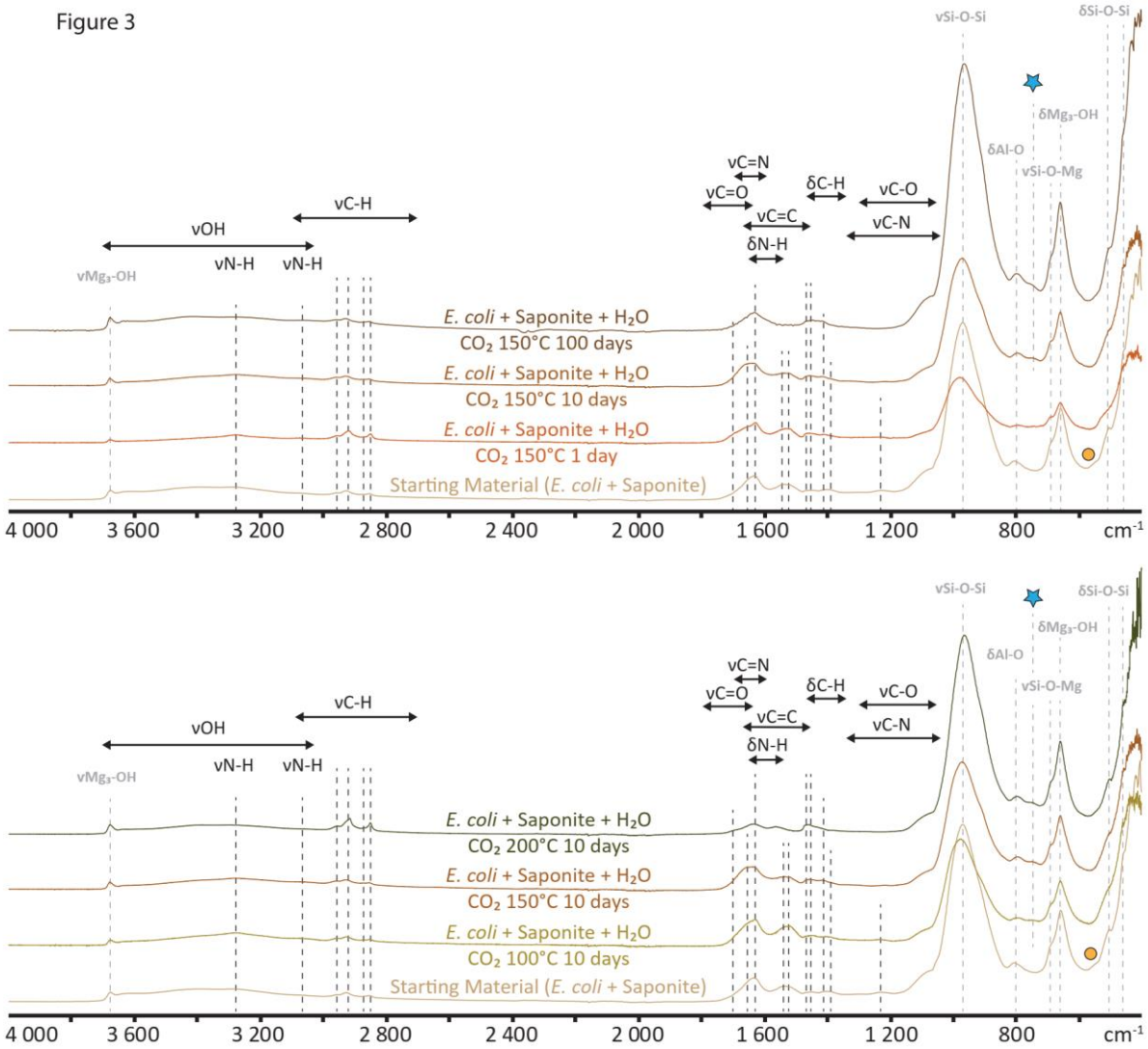

Figure 3. Mid-IR spectra of residues of experiments conducted in the presence of *E. coli* + saponite. The blue star at 750 cm^{-1} and the yellow circle at 530 cm^{-1} correspond to Si-O-Al or Al-OH or Mg-Al-OH vibrations and to Si-O-Mg vibrations, respectively. Note that the spectra of the starting materials (*E. coli* cells + pure saponite) and of the residue of the experiment conducted at 150°C for 10 days are shown twice to facilitate the comparison. All spectra are normalized to the CH band at 1465 cm^{-1}.

Figure 4

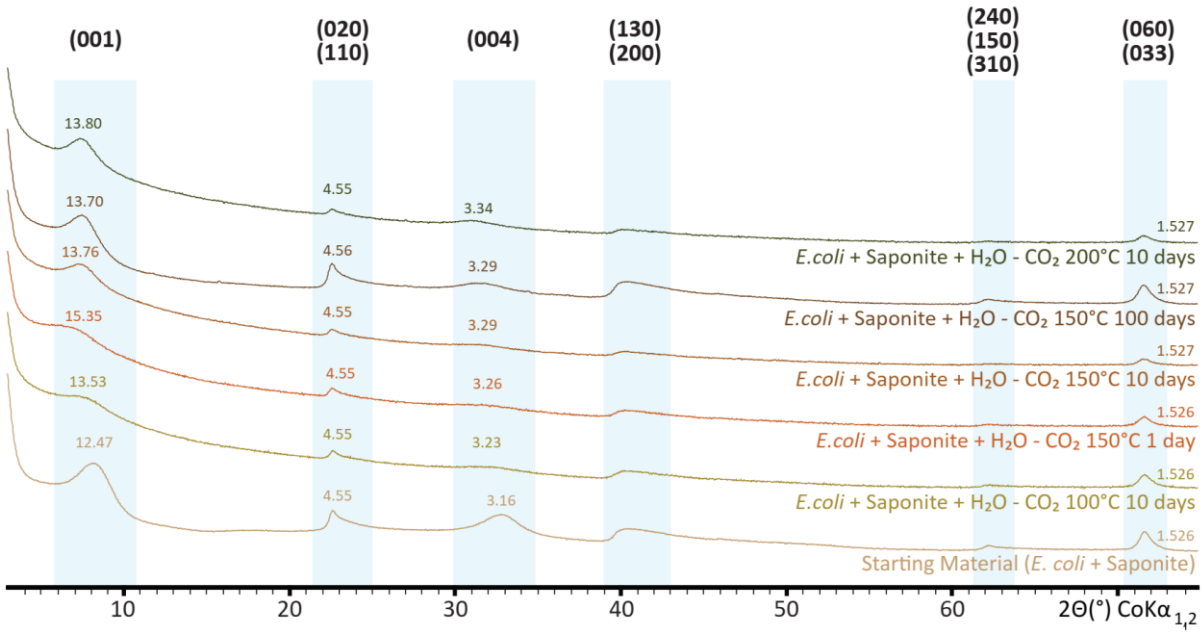

Figure 4. Powder XRD patterns of residues of experiments conducted in the presence and absence of *E. coli* cells.

Figure 5

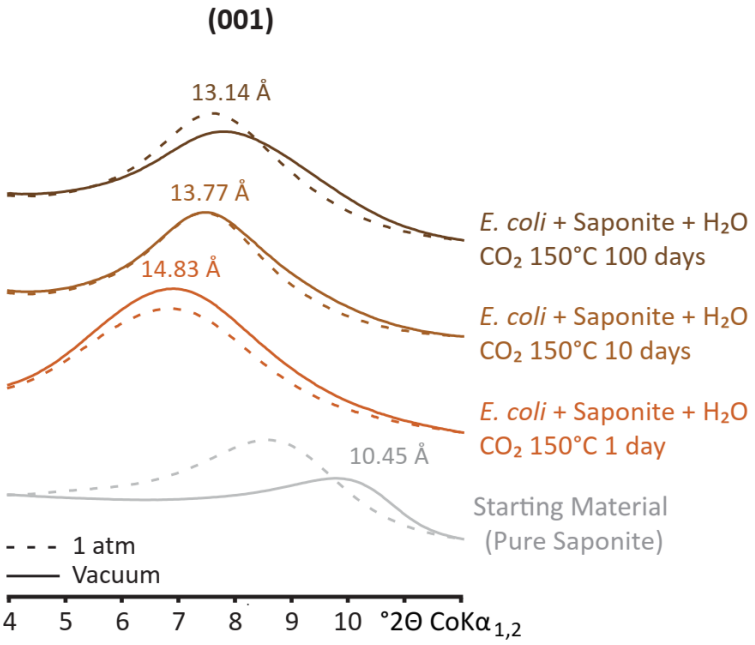

Figure 5. XRD patterns collected at 1 atmosphere and under vacuum on oriented preparations of the residues of experiments conducted with *E. coli* cells in the presence of saponite at 150°C for different durations. The XRD patterns of the starting material (pure saponite) is shown for comparison.